nature communications

Article

https://doi.org/10.1038/s41467-024-53996-7

Improved safety of chimeric antigen receptor T cells indirectly targeting antigens via switchable adapters

Received: 30 August 2023

Accepted: 28 October 2024

Published online: 18 November 2024

Check for updates

Hyung Bae Park[1,2,3], Ki Hyun Kim[1,3], Ju Hwan Kim[4], Sang Il Kim[1,3], Yu Mi Oh[1], Miseung Kang[1,2], Seoho Lee[1,2], Siwon Hwang[1,2], Hyeonmin Lee[1,3], TaeJin Lee[4,5], Seungbin Park[5], Ji Eun Lee[1,3], Ga Ram Jeong[1,6], Dong Hyun Lee[7], Hyewon Youn[3,8], Eun Young Choi[2,9], Woo Chan Son[10], Sang J. Chung[5,11] ✉, Junho Chung[1,2,3,11] ✉ & Kyungho Choi[1,2,3,11] ✉

Chimeric antigen receptor T (CAR-T) cells show remarkable efficacy for some hematological malignancies. However, CAR targets that are expressed at high level and selective to tumors are scarce. Several strategies have been proposed to tackle the on-target off-tumor toxicity of CAR-T cells that arise from sub-optimal selectivity, but these are complicated, with many involving dual gene expression for specificity. In this study, we show that switchable CAR-T cells with a tumor targeting adaptor can mitigate on-target off-tumor toxicity against a low selectivity tumor antigen that cannot be targeted by conventional CAR-T cells, such as CD40. Our system is composed of anti-cotinine murine CAR-T cells and cotinine-labeled anti-CD40 single chain variable fragments (scFv), with which we show selective tumor killing while sparing CD40-expressing normal cells including macrophages in a mouse model of lymphoma. Simple replacement of the tumor-targeting adaptor with a suicidal drug-conjugated tag may further enhance safety by enabling permanent in vivo depletion of the switchable CAR-T cells when necessary. In summary, our switchable CAR system can control CAR-T cell toxicity while maintaining therapeutic efficacy, thereby expanding the range of CAR targets.

Chimeric antigen receptor-transduced T cells (CAR-T cells) are anti-tumor therapeutic T cells that carry an artificial receptor, CAR, in which an extracellular tumor-targeting antibody moiety is linked to the intracellular signaling domains[1]. A decade ago, CAR-T cells targeting CD19 began to show remarkable therapeutic efficacy for relapsed and/or refractory acute lymphoblastic leukemia (70–80% complete remissions) in clinical trials[2]. Since then, there has been a surge in CAR-T cell development against hematological malignancies, resulting in the FDA approval of six CAR-T cell products to date[3]. Nonetheless, most CAR-T cells approved by the FDA or used in clinical trials target a

[1]Department of Biochemistry and Molecular Biology, Seoul National University College of Medicine, Seoul, Republic of Korea. [2]Department of Biomedical Sciences, Seoul National University College of Medicine, Seoul, Republic of Korea. [3]Cancer Research Institute, Seoul National University College of Medicine, Seoul, Republic of Korea. [4]AbTis Co. Ltd., Suwon, Gyeonggi-do, Republic of Korea. [5]Department of Biopharmaceutical Convergence, School of Pharmacy, Sungkyunkwan University, Suwon, Gyeonggi-do, Republic of Korea. [6]Ticaros Inc., Seoul, Republic of Korea. [7]Department of Medical Science, AMIST, University of Ulsan College of Medicine, Asan Medical Center, Seoul, Republic of Korea. [8]Department of Nuclear Medicine, Cancer Imaging Center, Seoul National University Hospital, Seoul, Republic of Korea. [9]Institute of Human Environment Interface Biology, Seoul National University College of Medicine, Seoul, Republic of Korea. [10]Department of Pathology, University of Ulsan College of Medicine, Asan Medical Center, Seoul, Republic of Korea. [11]These authors jointly supervised this work: Sang J. Chung, Junho Chung, Kyungho Choi. ✉e-mail: sjchung@skku.edu; jjhchung@snu.ac.kr; khchoi@snu.ac.kr

limited number of antigens, such as CD19, CD20, CD22, and BCMA, expressed mostly on B cell- or plasma cell-lineage blood tumors[3]. One of the main reasons for this paucity is that most tumor antigens are not tumor-specific, but rather are enriched in tumors and expressed at low levels in normal tissues. Therefore, CAR-T cells against these antigens can attack normal tissues as well as tumors, eliciting a serious adverse side effect called on-target off-tumor toxicity[4]. This toxicity has been demonstrated in several CAR-T clinical trials against solid tumor targets, such as CAXI, HER2, and CEA[5–7]. Thus, the proper design of strategies to reduce on-target off-tumor toxicity would greatly expand the list of CAR targets and broaden the indications for CAR-T cell therapy.

Various strategies have been proposed to overcome on-target off-tumor toxicity. Many strategies use a dual CAR expression system to increase the tumor specificity of CAR-T cells. For example, SynNotch CAR-T cells require dual engagement of two independent tumor antigens for proper activation, using the first CAR for antigen recognition, which in turn induces expression of the other CAR used for CAR-T cell stimulation[8,9]. In Split CAR-T cells, the activation domains are split into two different CARs[10,11]. Or iCAR-T cells express both a stimulatory CAR against a tumor antigen and an inhibitory CAR against a normal tissue antigen, thereby suppressing CAR-T cell activation against normal tissues[12]. Other strategies to prevent the long-term toxicity of CAR-T cells include eliminating CAR-T cells using suicidal enzymes or receptors co-expressed with CAR, such as inducible caspase9[13] and truncated CD20[14] or EGFR[15]. However, all these strategies are rather complicated and require dual gene modification, which takes up much space in the gene-transfer vector and reduces the chances of incorporating other beneficial genes, such as cytokines and stimulatory receptors[16].

The switchable CAR-T cell system is another strategy to reduce CAR-T cell toxicity[16]. CAR-T cells are directed against a small epitope tag, such as chemicals and peptides. Only when the separate anti-tumor antibody moiety (adapter) coupled to this tag is present, the anti-tag CAR-T cells are activated. Initially, this strategy was designed for multi-antigen targeting with single CAR-T cells using multiple adapters simultaneously[17,18]. Soon after, it was realized that the degree of CAR-T cell activation could be controlled by adjusting the doses of adapters[19–21]. Toxicity control by switchable CAR-T cells has been validated for cytokine release syndrome, another major CAR-T cell toxicity[19,22]. However, evaluating its utility for preventing on-target off-tumor toxicity is difficult because most in vivo CAR-T cell experiments are performed with human CAR-T cells in xenogeneic mouse models, and the human CAR cannot recognize murine target antigens in normal mouse tissues.

In this study, we took advantage of a murine syngeneic CAR-T cell therapy model to evaluate whether a switchable CAR system can be utilized for a tumor antigen that cannot be targeted by conventional CAR-T cells due to on-target off-tumor toxicity. The tumor antigen used is CD40, which is known to be expressed in various tumors, such as lymphoma, multiple myeloma, and acute myelocytic leukemia[23]. CD40 is also expressed on various immune cells, such as monocytes, macrophages, and dendritic cells, for which it acts as a stimulatory receptor[24]. Hence, antagonistic or agonistic anti-CD40 antibodies have been tested as anti-tumor immunotherapeutic modalities[25,26]. However, CD40 is also expressed on various non-hematopoietic normal cells, such as endothelial and parenchymal cells, raising concerns about normal tissue toxicity of CD40-targeting strategies[27–29].

Here we show that CD40-targeting conventional CAR-T cells cause lethal on-target off-tumor toxicity. In contrast, switchable CAR-T cells against CD40 do not show overt toxicity, but rather remarkable therapeutic efficacy against CD40-expressing tumors. On the other hand, when CAR-T cells must be eliminated to prevent long-term toxicity, a cytotoxic drug-conjugated tag instead of a tumor-targeting adapter can act as a suicidal switch for CAR-T cells without additional genetic modification. Thus, without a complicated CAR construct design, adjusting the dose of tumor-targeting adapters or changing them to suicidal drug conjugates for switchable CAR-T cells can regulate CAR-T cell toxicity and/or permanently eliminate unnecessary CAR-T cells.

Results

CD40 CAR-T cells show lethal toxicity in a murine CAR-T cell therapy model

To evaluate the efficacy and toxicity of anti-CD40 CAR-T cells (CD40 CAR-T cells) in a physiological setting, we designed a mouse syngeneic CAR-T cell therapy model. An anti-mouse CD40 single chain variable fragment (scFv) clone (C1C02) that binds both recombinant and cell surface-expressed CD40 was isolated from immunized chickens (Supplementary Fig. 1). Murine CAR-T cells were generated by retroviral transduction of Balb/C T cells with a CAR construct including C1C02 linked to a murine CD28/CD3zeta CAR backbone (Fig. 1a). The CAR-T cells properly expressed CAR on the surface and exhibited potent in vitro antitumor toxicity and cytokine production against A20, a mouse CD40(+) B-cell lymphoma cell derived from Balb/C mice. (Fig. 1b–d). Thus, the murine CD40 CAR-T cells were fully functional in vitro.

Next, to evaluate in vivo anti-tumor efficacy, CD40 CAR-T cells were transferred into A20 tumor-bearing Balb/C mice. Surprisingly, CAR-T cell-treated mice lost body weight rapidly and died within a few days (Fig. 1e, f). As this lethality far preceded tumor-induced lethality, CAR-T cell-induced acute toxicity was strongly suspected. Consistently, serum IL-6, a well-known biomarker of acute CAR-T cell toxicity such as cytokine release syndrome[30], was significantly elevated in CAR-T cell-treated mice (Fig. 1g). Since CD40 is known to be expressed in various normal tissues, this CAR toxicity may have been against endogenous CD40 rather than tumor-expressed CD40. Therefore, we investigated whether CAR-T cell toxicity occurs in the absence of a tumor in normal mice. The CAR-T cell-treated non-tumor-bearing mice showed a similar degree of toxicity (weight loss, lethality, and serum IL-6 elevation) to the tumor-bearing mice (Fig. 1h–j). In contrast, this toxicity was completely abolished in CD40-deficient mice (Fig. 1k–m). In the absence of toxicity in these mice, CD40 CAR-T cells now tended to exhibit anti-tumor efficacy (Supplementary Fig. 2). Thus, the conventional CD40 CAR-T cells induce on-target off-tumor toxicity against endogenous CD40 in normal tissues, which could be lethal.

Both hematopoietic and non-hematopoietic expression of CD40 cause CAR-T cell toxicity

Next, we sought to identify CD40-expressing normal tissues that contribute to this toxicity. CD40 is well-known to be expressed in macrophages and dendritic cells. Because these cell types produce proinflammatory cytokines such as IL-6 and IL-1 upon CD40 engagement[24], and serum IL-6 levels correlated with CD40 CAR-T cell toxicity as described above, we hypothesized that the CD40 CAR-T cells might engage CD40 on these cells and trigger their production of IL-6/IL-1, resulting in toxicity. When peritoneal macrophages or splenic dendritic cells were incubated with CD40 CAR-T cells in vitro, IL-6 and IL-1 secretion was profoundly increased compared to unstimulated cells (Fig. 2a and Supplementary Fig. 3). Of note, macrophages produced much more cytokines than dendritic cells. Since A20 tumor cells produced significantly less IL-6 and IL-1 in the same co-culture experiment (Fig. 2a), most of the IL-6 and IL-1 in the serum of CAR-T cell-treated mice is most likely produced by these innate immune cells.

It has been reported that IL-6 and IL-1 produced by macrophages are responsible for CAR-T cell toxicity, which is alleviated by their neutralization by antagonists[31,32]. Therefore, we investigated whether neutralization of the cytokines could alleviate CD40 CAR-T cell toxicity. Treatment with the anti-IL-6 or IL-1 antagonist, anakinra, did not prevent weight loss or lethality in mice treated with high-dose CAR-T cells (5×10^6 cells) (Fig. 2b and Supplementary Fig. 4a). However, in

https://doi.org/10.1038/s41467-024-53996-7

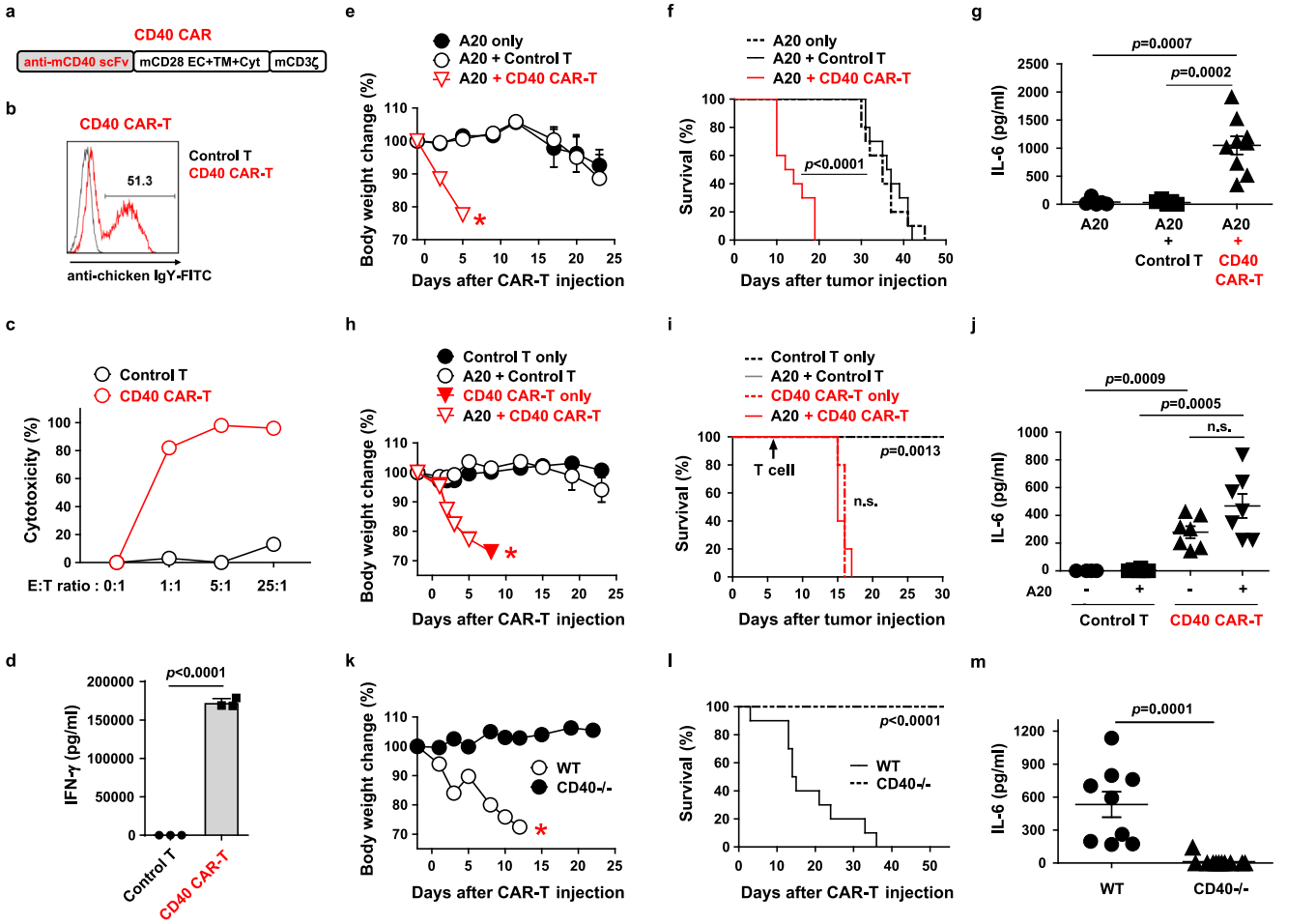

Fig. 1 | Murine CD40 CAR-T cells show lethal on-target off-tumor toxicity in a syngeneic lymphoma model. a Schematic diagram of the murine CD40 CAR construct. EC, extracellular; TM, transmembrane; Cyt, cytoplasmic domain. **b** Representative flow cytometry plot of CD40 CAR expression on mouse T cells 4 days after transduction. **c** Cytotoxicity of CD40 CAR-T cells against A20 cells. **d** IFN-γ production after co-culture of control T cells or CD40 CAR-T cells with A20 cells for 24 h, measured in triplicate. Results are representative of three independent experiments (**c**, **d**). **e**–**g** Balb/C mice were injected *i.v.* with A20-Luc cells (1×10^6) on day 0, irradiated (2.5 Gy) for lymphodepletion on day 6, and injected *i.v.* with control T or CD40 CAR-T cells (5×10^6) on day 7. Body weight change (**e**, $n = 5$) and survival (**f**, $n = 10$) were measured. Serum levels of IL-6 were measured three days after T cell injection (**g**, $n = 9$). Each dot represents the value of a single mouse. **h**–**j** The same experiments as in **e**–**g** were performed including the groups not injected with A20-Luc cells. Body weight change (**h**, $n = 5$), survival (**i**, $n = 5$), and serum levels of IL-6 (**j**, $n = 7$) were measured. **k**–**m** Wild-type and CD40 knockout B6 mice were irradiated (3 Gy) on day 6 and injected *i.v.* with CD40 CAR-T cells (5×10^6) on day 7. Body weight change (**k**, $n = 5$), survival (**l**, $n = 10$), and serum levels of IL-6 (**m**, $n = 9$) were measured. Measurements of body weight were halted when the mice began to die (red asterisks in **e**, **h**, **k**). Data in (**e**, **h**, **i**, and **k**) are representative of at least two independent experiments. Data in (**f**, **g**, **j**, **l**, and **m**) are pooled from two replicate experiments. Data in (**d**, **e**, **g**, **h**, **j**, **k**, and **m**) are presented as mean ± SEM. Statistical significance was determined by either the log-rank (Mantel-Cox) test (**f**, **i**, **l**) or the unpaired two-tailed *t* test (**d**, **g**, **j**, **m**). *p*: *p*-value, n.s.: not significant. Source data are provided in the Source Data file.

mice treated with sublethal low-dose CAR-T cells (1×10^6 cells), anti-IL-6 treatment resulted in a more rapid, partial reversal of CAR-T cell-induced body weight loss (Fig. 2c and Supplementary Fig. 4b). Anakinra alone or in combination with anti-IL-6 did not facilitate this recovery. Blockade of another potential toxic cytokine, IL-12, in combination with anti-IL-6 and anakinra did not prevent the lethal toxicity of the high-dose CAR-T cells, nor did it further reduce the sublethal toxicity of the low-dose CAR-T cells compared to anti-IL-6 and anakinra treatment (Supplementary Fig. 5).

Since macrophages are the main producers of IL-6, we also tried macrophage depletion by clodronate treatment. Intraperitoneal injection of clodronate efficiently eliminated macrophages (Supplementary Fig. 6). Although this treatment did not prevent weight loss and lethality in the high-dose CAR-T cell-treated mice, it showed a faster, partial recovery of weight loss in the low-dose CAR-T cell-treated mice (Fig. 2d, e and Supplementary Fig. 4c, d). Consistently, serum IL-6 levels were significantly reduced by macrophage depletion (Fig. 2f). Thus, IL-6, most likely produced by macrophages, partially contributed to CD40 CAR-T cell toxicity, albeit IL-6 neutralization alone cannot block lethal toxicity.

Since hematopoietic cells such as macrophages were not fully responsible for the lethality, we checked whether non-hematopoietic expression of CD40 contributed to the toxicity. To differentiate the non-hematopoietic and hematopoietic expression of CD40 in mice, we performed bone marrow chimera experiments using CD40 knockout mice. When CD40 is expressed exclusively in hematopoietic tissues in mice (lethally irradiated CD40 knockout mice reconstituted with wild-type bone marrow), CD40 CAR-T cells resulted in partial weight loss, but not lethality, consistent with the partial toxicity mediated by macrophages as described above (Fig. 2g, h). On the other hand, when CD40 is expressed exclusively in non-hematopoietic tissues in mice (lethally irradiated wild-type mice reconstituted with CD40 knockout bone marrow), CD40 CAR-T cells elicited profound weight loss and lethality comparable to that in wild-type control mice. Thus, non-hematopoietic CD40 expression is largely responsible for the lethal toxicity of CAR-T cells.

https://doi.org/10.1038/s41467-024-53996-7

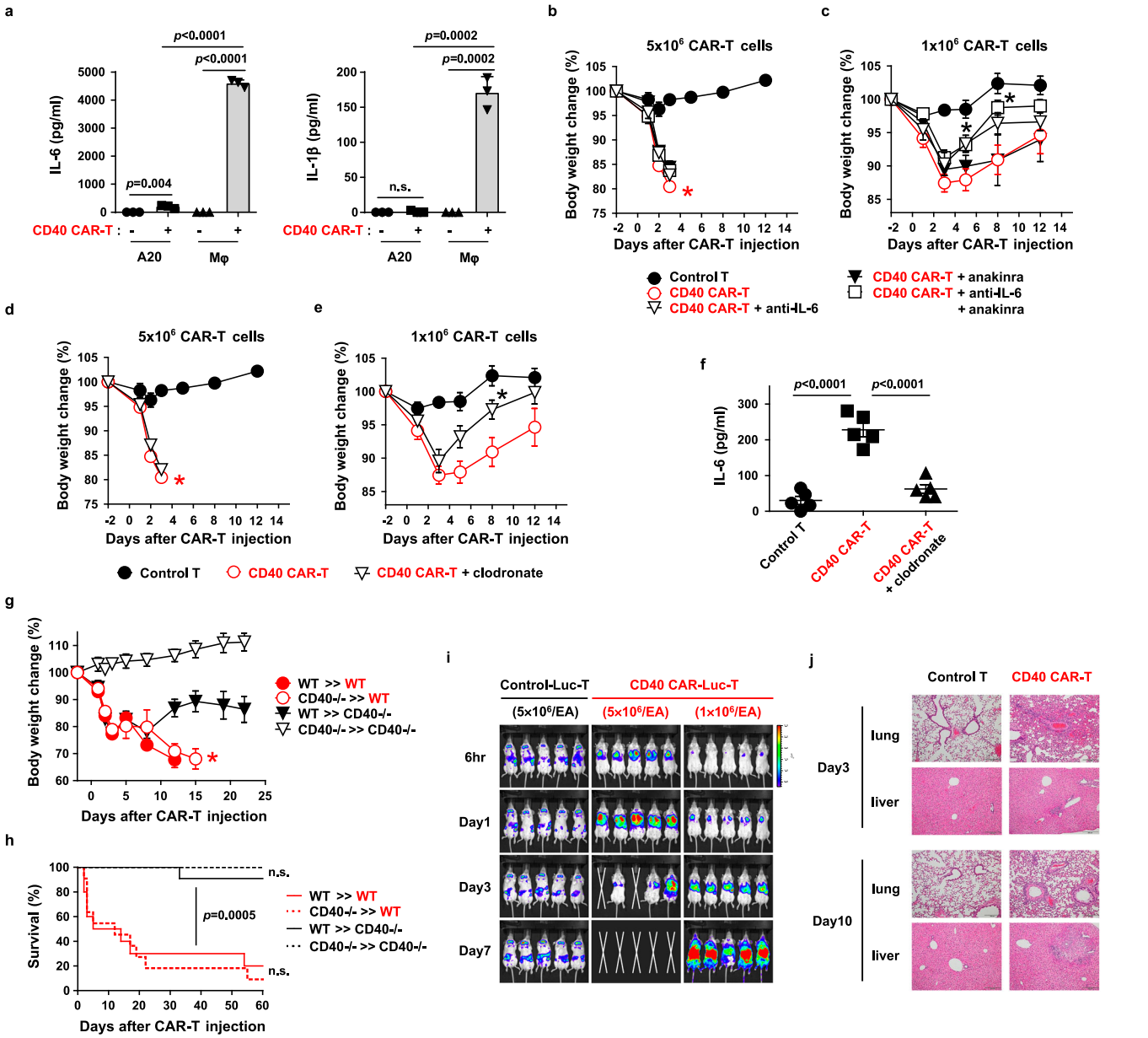

Fig. 2 | Both hematopoietic and non-hematopoietic expression of CD40 contribute to on-target off-tumor toxicity. a Production of IL-6 or IL-1β after co-culture of CD40 CAR-T cells with A20 or peritoneal macrophages (Mφ) for 24 h, measured in triplicate. Results are representative of three independent experiments. **b**–**f** Balb/C mice were irradiated (2.5 Gy) for lymphodepletion on day -1 and injected with 5×10^6 (**b**, **d**, **f**) or 1×10^6 (**c**, **e**) control T cells or CD40 CAR-T cells on day 0. IL-6 or IL-1β neutralization (**b**, **c**) and phagocyte depletion (**d**–**f**) were performed as described in "Methods". Body weight change (**b**–**e**, $n = 5$) and serum levels of IL-6 (**f**, $n = 5$) were measured. Each dot in (**f**) represents the value of a single mouse. *: $p = 0.0211$ on day 5, $p = 0.0187$ on day 8 (**c**), and $p = 0.0029$ on day 8 (**e**), compared to CD40 CAR-T group. **g**, **h** BM chimeras were established (e.g., CD40-/-»WT denotes the transfer of donor BMs from CD40-knockout mice to B6 wild-type recipients). After 8 weeks, chimeric mice were irradiated (2.5 Gy) on day -1 and injected with CD40 CAR-T cells (5×10^6) on day 0. Body weight change (**g**, $n = 5$) and survival (**h**, $n = 10$) were measured. *p* for WT»CD40-/- versus WT»WT (**h**). **i** Balb/C mice were irradiated (2.5 Gy) on day -1 and injected with GFP-efflux T (control-Luc-T) or CD40 CAR-efflux T cells (CD40 CAR-Luc-T) (5 or 1×10^6) on day 0. In vivo, the distribution of injected T cells was visualized by bioluminescence imaging. **j** Histology of lung and liver was examined by H&E staining 3 and 10 days after CAR-T (1×10^6) injection (100× magnification, scale bar: 200 μm). Measurements of body weight were halted when the mice began to die (red asterisks in **b**, **d**, **g**). Data in (**h**) are pooled from two replicate experiments. All other data are representative of at least two independent experiments. Data in **a**–**g** are presented as mean ± SEM. Statistical significance was determined by 1-way ANOVA (**c**, **e**), unpaired two-tailed *t* test (**f**), or log-rank (Mantel-Cox) test (**h**). *p*: *p*-value, n.s.: not significant. Source data are provided in the Source Data file.

We then wanted to evaluate which tissues CD40 CAR-T cells target for lethality. To trace the CAR-T cell migration and accumulation in vivo, we generated a retroviral vector carrying both CD40 CAR and the enhanced luciferase (effluc) gene, allowing kinetic bioluminescence imaging of CD40 CAR-T cells in live mice. While control effluc-transduced T cells without CAR initially migrated to the spleen and dispersed to various organs in low numbers (low bioluminescence signal), CD40 CAR-T cells rapidly and gradually accumulated in the lung followed by death of the mice at a high dose of CAR-T cells (Fig. 2i). At a low dose of CAR-T cells, CAR-T cells accumulated in the lung with delayed kinetics and subsequently spread throughout the body with increased cell expansion (high bioluminescence signal). Histologically, while control mice showed no tissue inflammation, CAR-T cell-treated mice showed severe

https://doi.org/10.1038/s41467-024-53996-7

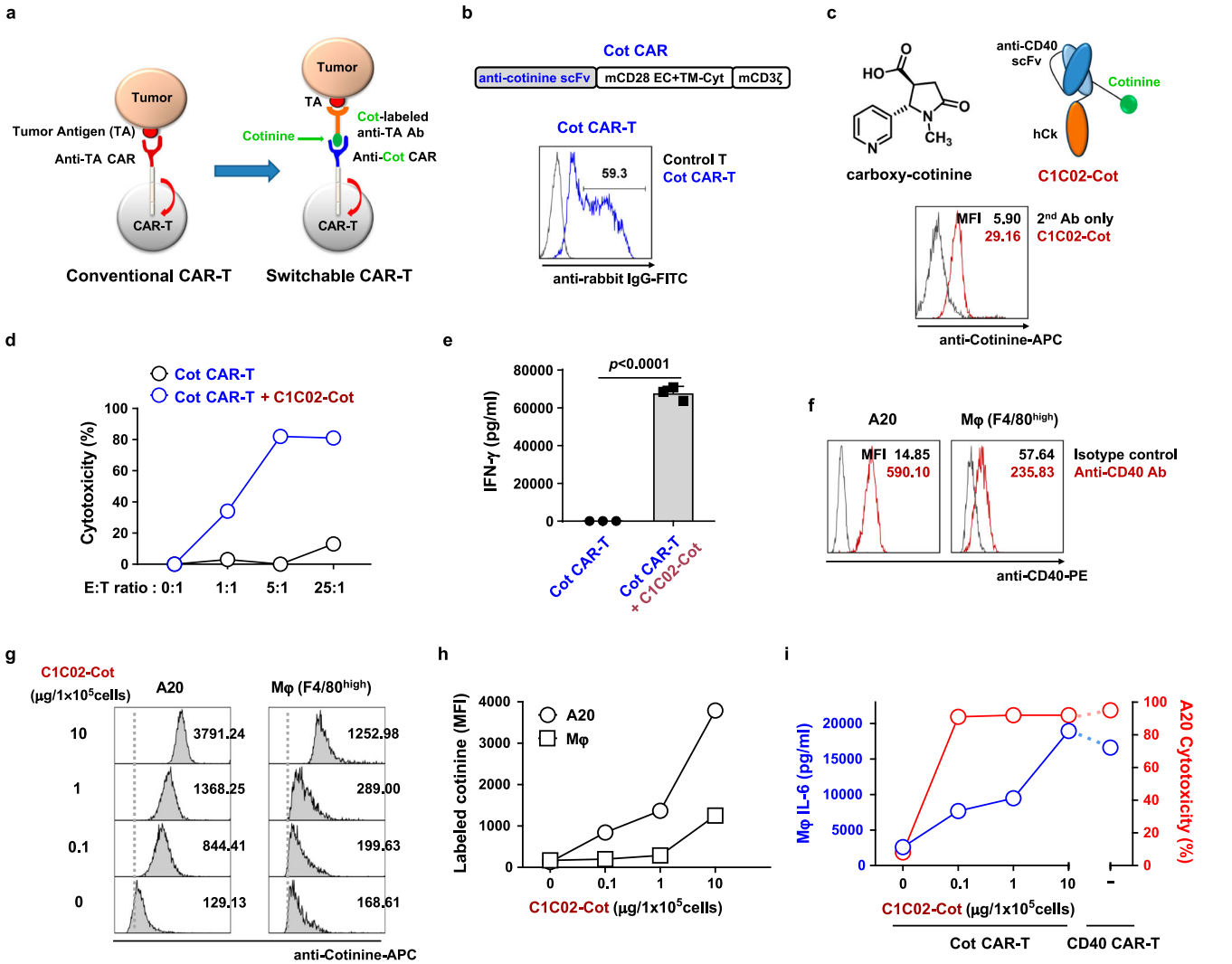

Fig. 3 | Cotinine-labeled anti-CD40 scFv can be used as a dose-adjustable adapter for switchable Cot CAR-T cells in vitro. a Scheme of conventional CAR-T and switchable CAR-T cells. **b** Schematic diagram of the murine Cot CAR construct and a representative flow cytometry plot of Cot CAR expression on mouse T cells 4 days after transduction. **c** Chemical structure of carboxy cotinine (top left). Schematic diagram of cotinine-labeled anti-mouse CD40 scFv-Cκ (C1C02-Cot) (top right). Representative flow cytometry plot of binding of C1C02-Cot to A20 cells (bottom). **d** Cytotoxicity of Cot CAR-T cells against A20 cells preincubated with C1C02-Cot. **e** IFN-γ production after co-culture of Cot CAR-T cells with A20 cells preincubated with C1C02-Cot for 24 h, measured in triplicate. Data are presented as mean ± SEM. Statistical significance was determined by an unpaired two-tailed *t* test. Results are representative of three independent experiments (**d**, **e**). **f** CD40 expression levels in A20 cells and F4/80 (+) peritoneal macrophages (Mφ) as determined by staining with a commercially available anti-mouse CD40 antibody. **g**, **h** Comparison of dose-dependent cell binding affinity of C1C02-Cot between A20 and macrophage. Mean fluorescence intensities (MFIs) of binding are shown as values within the plot (**g**) and as a graph (**h**). **i** For toxicity readouts, macrophages were preincubated with various concentrations of C1C02-Cot and co-cultured with Cot CAR-T or CD40 CAR-T cells for 24 h. The amount of IL-6 in culture supernatants was measured (mean ± SEM, left axis and blue lines). For efficacy readouts, A20 cells (target) were preincubated with various concentrations of C1C02-Cot and then co-cultured with Cot CAR-T cells (effector) at an E:T ratio of 5:1 for 6 h. CD40 CAR-T cells were co-cultured with target cells not treated with C1C02-Cot. Percent cytotoxicity was calculated from flow cytometry-based viable cell counting (right axis and red lines). Results in **g**–**i** are representative of at least two independent experiments. *p*: *p*-value. Source data are provided in the Source Data file.

perivascular inflammation in the lung initially (day 3) and progressive liver necrosis later (day 10) (Fig. 2j). Extensive extramedullary hematopoiesis in the red pulp of the spleen was also observed on day 10 (Supplementary Fig. 7). Other organs such as intestine and kidney were spared. Consistently, high levels of CD40 mRNA were detected in lung and spleen, and C1C02 scFv protein bound to lung endothelium and leukocytes in the red pulp of the spleen (Supplementary Fig. 8). It was also found that CD40 mRNA was enriched in vascular cells among various cell types in the lung (Supplementary Fig. 9). Therefore, tissue damage by CD40 CAR-T cells was highly correlated with CD40 expression, although liver inflammation was likely caused by portal vein infarction, as CD40 expression in liver parenchyma was not high.

Thus, both hematopoietic and non-hematopoietic expression of CD40 contributed to CD40 CAR-T cell toxicity, which could not be avoided in the conventional CAR therapy model.

Separation of efficacy and toxicity using a switchable CAR system with cotinine-labeled adapters

A switchable CAR system has been proposed as a tool to avoid acute toxicities such as cytokine release syndrome. Therefore, we examined whether the on-target off-tumor toxicity of CD40 CAR-T cells could be overcome by this strategy. To this end, we set up a CAR against a chemical tag, cotinine, together with a cotinine-tagged antibody as a tumor-targeting adapter (Fig. 3a). Cotinine is an inert metabolite of nicotine that has been used as an epitope tag for anti-cotinine

antibodies for various applications and recently for anti-cotinine switchable CAR-NK cells[33–36]. Therefore, anti-cotinine murine CAR-T cells (Cot CAR-T cells) were generated using a retroviral vector harboring an anti-cotinine scFv linked to a CD28/CD3zeta-based CAR backbone (Fig. 3b). The switchable CAR function of Cot CAR-T cells was successfully validated by co-culture with HER2- or CD20-expressing tumor cell lines together with cotinine-labeled anti-HER2 or anti-CD20 antibodies, respectively (Supplementary Fig. 10). We then generated a cotinine-labeled anti-mouse CD40 adapter (CD40 adapter), C1C02 scFv fused with the constant region of the human immunoglobulin kappa light chain (Cκ) (Fig. 3c). To ensure single cotinine labeling per adapter molecule (drug-to-antibody ratio, DAR 1), a cysteine residue was introduced into the framework region of the scFv to allow maleimide linker-mediated monomeric cotinine conjugation[37]. The cotinine-conjugated CD40 adapter bound to A20 tumor cells, and mediated Cot CAR-T cell-dependent tumor cell cytotoxicity and CAR-T cell activation in vitro (Fig. 3c–e). Therefore, the cotinine-mediated switchable CAR system was well established.

CAR-T cells require strong antigen engagement for activation, and the expression level of a tumor antigen is usually higher in tumor cells than in normal cells. Therefore, it can be postulated that adjusting the adapter dose in a switchable CAR system would allow finding an optimal adapter dose range that does not elicit toxicity to normal cells and yet induces sufficient tumor cell killing (Supplementary Fig. 11). To test this concept in vitro, we chose macrophages as a normal cell type because macrophages express CD40 and we have already observed that macrophages produce the toxic cytokine IL-6 upon co-incubation with CD40 CAR-T cells (Fig. 2a). In this case, IL-6 production by macrophages may be a sensitive indicator of CAR-T cell-mediated toxicity on macrophages in co-culture experiments. To this end, we co-cultured Cot CAR-T cells with either normal macrophages or A20 tumor cells treated with different doses of the cotinine-tagged adapters. IL-6 production by macrophages was used as a readout for normal cell toxicity, and cytotoxicity against A20 as a readout for anti-tumor efficacy. As expected, A20 tumor cells expressed CD40 on the cell surface at much higher levels than macrophages (Fig. 3f). Consistent with this, tumor cells showed much stronger adapter binding than macrophages at all CD40 adapter doses. In particular, at the doses where macrophages bound the adapter very weakly (1 and 0.1 μg/10^5 cells), tumor cells still bound the adapter at significant levels (Fig. 3g, h). In terms of toxicity, macrophages treated with the highest dose (10 μg/10^5 cells) secreted IL-6 at levels similar to those co-cultured with conventional CD40 CAR-T cells, suggesting that the highest dose represents a toxic level of the adapter (Fig. 3i). However, at 10- to 100-fold lower doses of the adapter (1 and 0.1 μg/10^5 cells), the amount of IL-6 secreted decreased significantly, indicating reduced toxicity. Interestingly, on the efficacy side, Cot CAR-T cells with these low doses of adapter (1 and 0.1 μg/10^5 cells) still showed the equivalent level of tumor cell killing as Cot CAR-T cells with the highest dose of adapter (10 μg/10^5 cells) and as conventional CD40 CAR-T cells (Fig. 3i). We also investigated the cytotoxicity of CAR-T cells on macrophages. Consistently, CD40 CAR-T cells showed cytotoxicity on macrophages equivalent to that on tumor cells. However, Cot CAR-T cells with adapters exhibited significantly less cytotoxicity on macrophages than on tumor cells (Supplementary Fig. 12a). A similar differential cytotoxicity of CAR-T cells was observed on dendritic cells, which also express CD40 (Supplementary Fig. 12b). Interestingly, the surviving dendritic cells cultured with Cot CAR-T cells and adapters were partially stimulated, as demonstrated by increased expression of activation markers such as CD80 and CD86, suggesting a partial immunostimulatory effect of anti-CD40 adapters coupled with Cot CAR-T cells (Supplementary Fig. 12c, d). Thus, Cot CAR-T cells equipped with moderate to low doses of adapter are fully competent to kill tumors, but have a much lower potential to cause normal cell toxicity, implying that the optimal adapter dose window exists to maintain efficacy without significant toxicity.

Cot CAR-T cells with adapter show anti-tumor efficacy without overt toxicity in vivo

To evaluate whether this idea of efficacy and toxicity dissociation is indeed possible in vivo, Cot CAR-T cells were injected into A20-bearing mice together with cotinine-tagged CD40 adapters. Adapters used in switchable CAR systems are typically small antibody fragments, such as scFv or Fab, that have a short serum half-life enabling rapid switching on and off of CAR-T cell activity. These adapters are infused repeatedly during the effector phase of CAR-T cell therapy to maintain CAR-T cell activity. In this study, we followed a regular adapter treatment dose and schedule of switchable CAR-T cells used to regulate cytokine release syndrome: 20 μg of adapter injected eight times every two days (Fig. 4a)[19,38]. In contrast to the rapid weight loss and death of mice treated with conventional CD40 CAR-T cells, mice treated with Cot CAR-T cells and the CD40 adapter experienced transient and mild weight loss but regained normal weight within a few days, and all survived (Fig. 4b). Consistently, the serum toxicity biomarker IL-6 was not elevated in Cot CAR-T cell-treated mice, unlike CD40 CAR-T cell-treated mice (Fig. 4c). Next, we evaluated anti-tumor efficacy by bioluminescence imaging of luciferase-expressing A20 cells. To our surprise, tumor burden was drastically reduced by co-treatment of Cot CAR-T cells and the adapters (Fig. 4d, e). This anti-tumor effect of Cot CAR-T cells and adapters was due to direct cytotoxicity on CD40 on tumor cells rather than a partial immunostimulatory effect shown in vitro (Supplementary Fig. 12c, d) because the elimination of CD40 on A20 cells abolished the anti-tumor efficacy (Supplementary Fig. 13). The absence of acute lethality of Cot CAR-T cells with the CD40 adapter was also recapitulated in C57BL/6 (hereafter B6) mice inoculated with CD40-transduced EL4 lymphoma, although the therapeutic benefit in this model was moderate (Supplementary Fig. 14).

To further confirm whether Cot CAR-T cells bypass CD40-expressing normal tissues and migrate to the tumor tissue, we traced the luciferase-expressing CAR-T cells in tumor-bearing mice (Fig. 4f). In this case, we injected the tumors subcutaneously to localize the exact tumor sites. In contrast to the strong infiltration of conventional CD40 CAR-T cells into the lung, Cot CAR-T cells bypassed the lung, first accumulated in the spleen, and then migrated very specifically to the tumor sites. Of note, Cot CAR-T cells migrated to tumor sites even in the absence of the adapters, suggesting that the inflammation at the tumor sites may have recruited the CAR-T cells[39,40]. Consistently, in contrast to the severe tissue inflammation in mice treated with CD40 CAR-T cells, the normal tissues (lung, spleen, and liver) of mice treated with Cot CAR-T cells and CD40 adapter showed no leukocyte infiltration and inflammation (Supplementary Fig. 15). Taken together, the switchable Cot CAR-T cells were able to significantly reduce CD40-expressing tumor burden without on-target off-tumor toxicity, which cannot be avoided in conventional CD40 CAR-T cell therapy.

Switchable Cot CAR system can be used for human CAR-T cell therapy

We next sought to determine whether this therapeutic effect of anti-CD40 murine switchable CAR-T cells could be recapitulated in a human Cot CAR-T cell therapy model. Anti-cotinine scFv was linked to a human CD28/CD3zeta CAR backbone to generate an anti-cotinine human CAR retroviral construct (Fig. 5a). Anti-cotinine human CAR-T cells were produced by retroviral transduction of human peripheral blood T cells (hCot CAR-T cells) (Fig. 5b). For the adapters, we screened a new phage display scFv library prepared from human CD40-immunized chickens and selected a clone, 2B1, which was confirmed to bind both recombinant human CD40 proteins and cell surface CD40 (Supplementary Fig. 16). To

https://doi.org/10.1038/s41467-024-53996-7

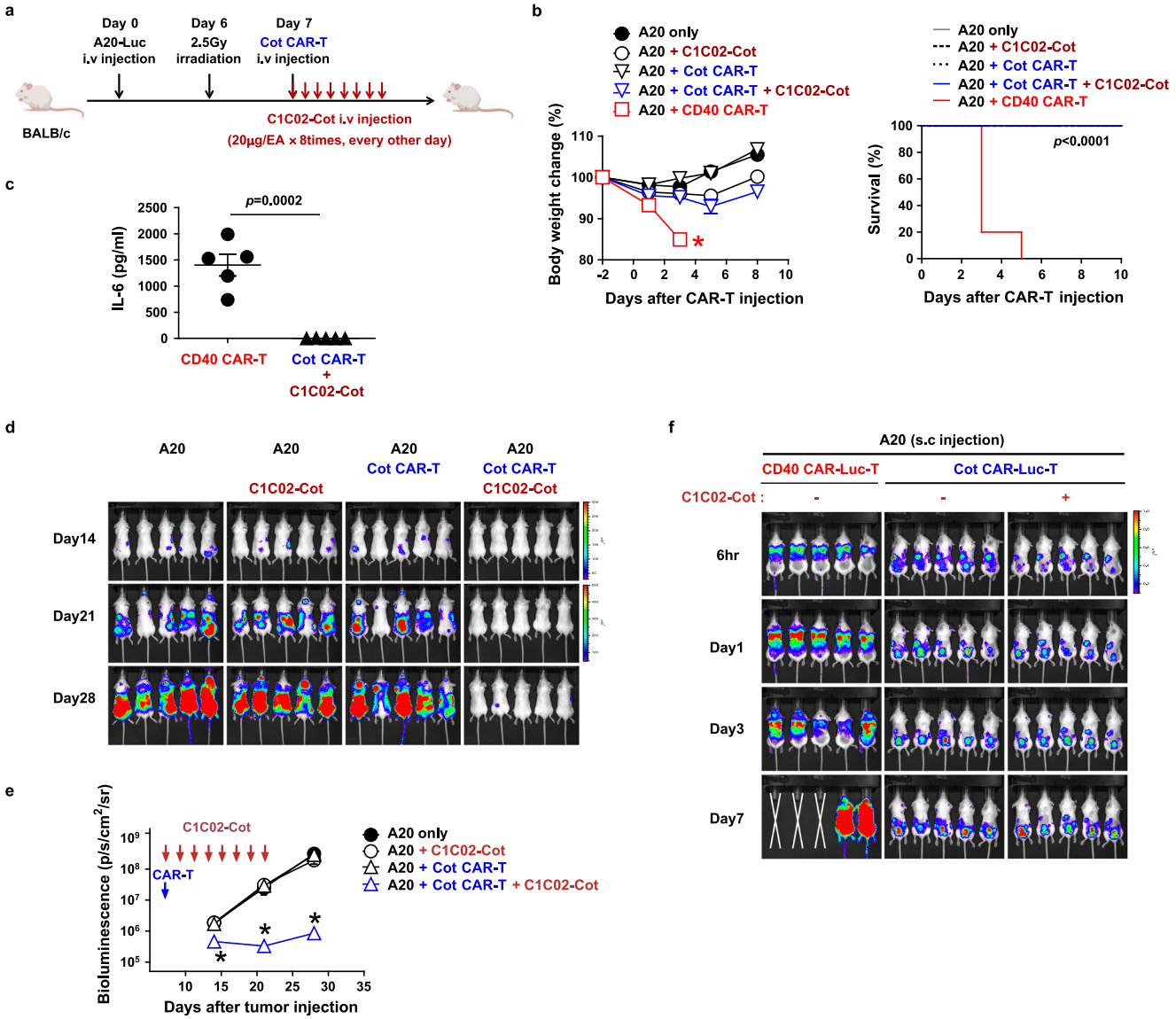

Fig. 4 | Anti-mouse CD40 switchable CAR-T cells eliminate lymphoma cells in vivo without overt toxicity. a Experimental scheme for the treatment of murine B-cell lymphoma using syngeneic Cot CAR-T cells. Balb/C mice were injected *i.v.* with A20-Luc cells (1×10^6) on day 0, irradiated (2.5 Gy) for lymphodepletion on day 6, and injected with Cot CAR-T cells (5×10^6) on day 7. From the day of CAR-T cell injection, C1C02-Cot (20 μg/head) was injected *i.v.* every other day for a total of 8 times. **b** Body weight change ($n = 5$) and survival ($n = 5$) were measured. Measurements of body weight were halted when the mice began to die (red asterisk). **c** Serum levels of IL-6 were measured 3 days after CAR-T injection ($n = 5$). Each dot represents the value of a single mouse. Statistical significance was determined by log-rank (Mantel-Cox) test (**b**) and unpaired two-tailed *t* test (**c**). **d**, **e** Bioluminescence imaging of tumor burden at indicated time points after A20-Luc cell injection (**d**). Bioluminescence intensity is calculated as the mean flux (p/s/cm²/sr) of a region of interest (ROI) in an individual mouse. Statistical significance between groups at each time point ($n = 5$) was determined by the nonparametric Kruskal-Wallis test (**e**). *: $p = 0.0172$ on day 14, $p = 0.011$ on day 21, and $p = 0.0115$ on day 28, compared to A20 only group. **f** In vivo CAR-T tracing using luciferase-expressing CAR-T cells and bioluminescence imaging. Balb/C mice were injected *s.c.* on the back with A20 cells. When tumor mass was detectable at the injection site, mice were irradiated (2.5 Gy) and injected the next day with CD40 CAR-Luc-T cells or Cot CAR-Luc-T cells (5×10^6) with or without C1C02-Cot injection every other day. Bioluminescence imaging was performed at the indicated time points after CAR-T cell injection. Data in (**b**, **c**, and **e**) are presented as mean ± SEM. Results are representative of at least three (**b**, **d**, **e**) or two (**c**, **f**) independent experiments. *p*: *p*-value. Source data are provided in the Source Data file.

use 2B1 as an anti-human CD40 adapter (hCD40 adapter), we conjugated cotinine to the framework region of scFv-Cκ as we did for the anti-mouse CD40 adapter. The binding of this adapter to the cell surface was confirmed by flow cytometry (Fig. 5b). The in vitro cytotoxicity and functional activity of hCot CAR-T cells in the presence of the hCD40 adapter was validated in co-culture with Daudi human CD40(+) lymphoma cells (Fig. 5c, d). To evaluate their efficacy in vivo, hCot CAR-T cells were injected into tumor-bearing (luciferase-transfected Daudi) immunodeficient NSG mice together with an infusion of hCD40 adapter every two days (Fig. 5e). Similar to the murine CAR-T cell model, hCot CAR-T cells co-infused with hCD40 adapter effectively reduced tumor burden compared to hCot CAR-T cells in the absence of adapter (Fig. 5f, g). Hence, the efficacy of CD40-targeting switchable Cot CAR-T cells was also validated in a human CAR system.

Cot CAR-T cells can be permanently eliminated by suicidal cotinine-drug conjugates

Although we have shown that the acute toxicity of CAR-T cells can be controlled by adjusting the dose of the adapter for switchable CAR-T cells, physical removal of CAR-T cells may be necessary to prevent

https://doi.org/10.1038/s41467-024-53996-7

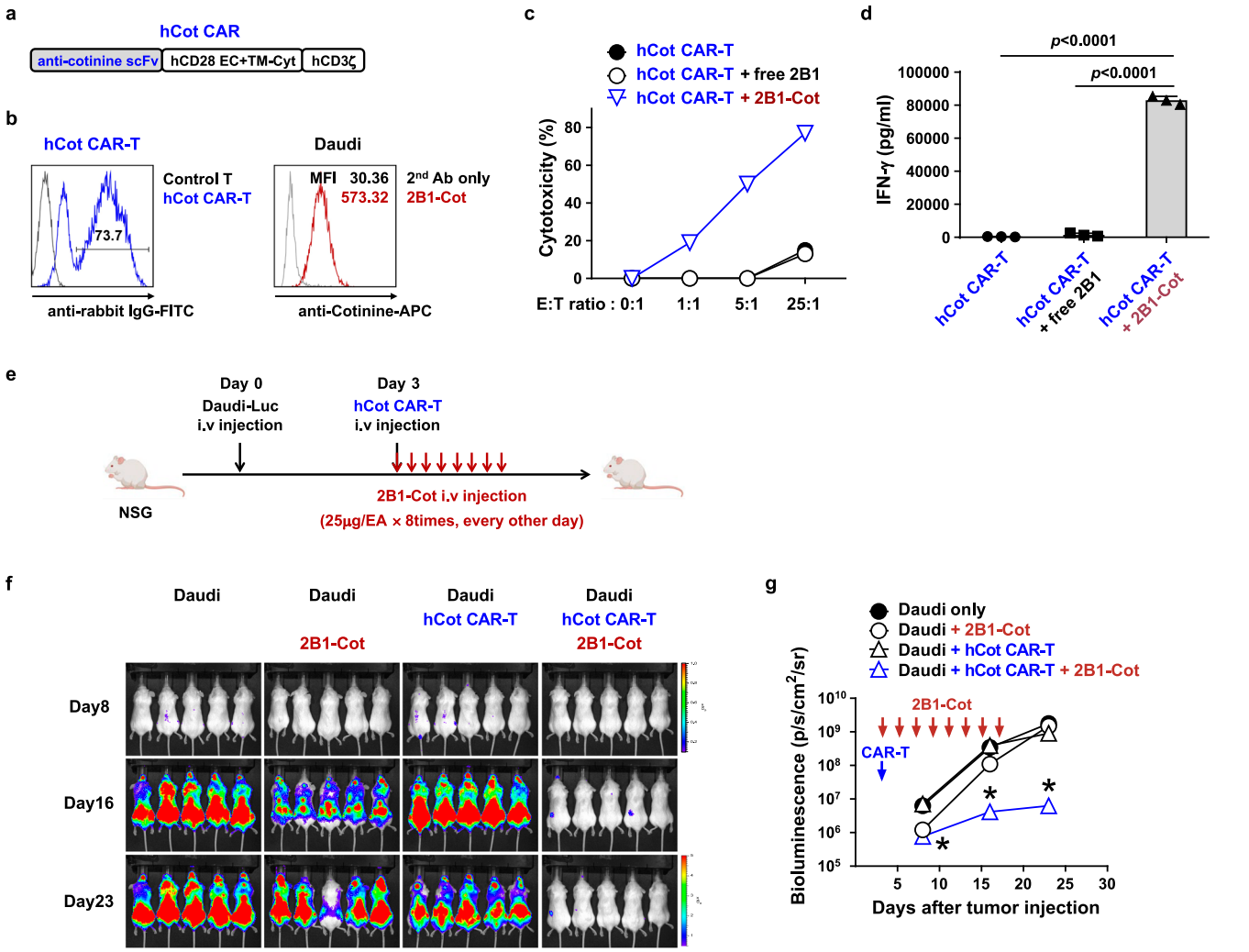

Fig. 5 | Anti-tumor efficacy of anti-CD40 switchable CAR-T cells is recapitulated with an anti-human CD40 adapter and human Cot CAR-T cells in vivo. **a** Schematic diagram of the hCot CAR construct. **b** Representative flow cytometry plot of Cot-CAR expression on human T cells 5 days after transduction (left); cotinine-labeled 2B1-Cκ (2B1-Cot) binding to Daudi cells (right). **c** Cytotoxicity of hCot CAR-T cells against Daudi cells preincubated with 2B1-Cκ (free 2B1) or 2B1-Cot. **d** IFN-γ production after co-culture of hCot CAR-T cells with Daudi cells pre-incubated with free 2B1 or 2B1-Cot for 24 h, measured in triplicate. Statistical significance was determined by an unpaired two-tailed *t* test. Results are representative of three independent experiments (**c**, **d**). **e** Experimental scheme for the treatment of human B-cell lymphoma xenografts with hCot CAR-T cells. NSG mice were injected *i.v.* with Daudi-Luc cells (5×10^5) on day 0 and hCot CAR-T cells (1×10^7) on day 3. From the day of CAR-T cell injection, 2B1-Cot (25 μg/head) was injected *i.v.* every other day for a total of 8 times. **f**, **g** Bioluminescence imaging of tumor burden at the indicated time points after Daudi-Luc cell injection (**f**). Bioluminescence intensity is calculated as the mean flux (p/s/cm²/sr) of a region of interest (ROI) in an individual mouse (**g**). Statistical significance between groups at each time point ($n = 5$) was determined by the nonparametric Kruskal-Wallis test. *: $p = 0.0019$ on day 8, $p = 0.001$ on day 16, and $p = 0.0025$ on day 23, compared to Daudi only group. Results are representative of at least two independent experiments. Data in (**d** and **g**) are presented as mean ± SEM. *p*: *p*-value. Source data are provided in the Source Data file.

long-term toxicities such as malignant transformation of CAR-T cells or delayed graft-versus-host disease (GVHD) by allogeneic CAR-T cells. The previously proposed strategies to eliminate CAR-T cells are co-expression of suicidal receptor or enzyme genes with the CAR gene in T cells, which occupies a significant space in the retroviral transfer vector. Here, we designed a strategy to eliminate Cot CAR-T cells without further gene modification by simply replacing the tumor-targeting adapter with a suicidal adapter; cytotoxic drug-labeled cotinine (Fig. 6a). As a suicidal adapter, we generated cotinine-labeled saporin (Cot-saporin) by complexing chemically synthesized biotin-conjugated cotinine with streptavidin-saporin (Fig. 6b and Supplementary Fig. 17). Saporin is a ribosome-inactivating toxin protein from a plant, and streptavidin-saporin has been used for several immunotoxins to deplete hematopoietic stem cells and T cells in preclinical studies[41–44]. First, we investigated this concept in vitro by incubating murine Cot CAR-T cells with various doses of Cot-saporin. As expected, Cot-saporin showed dramatic cytotoxicity to Cot CAR-T cells at doses that were not cytotoxic to CAR-non-expressing T cells (bystander T cells) (Fig. 6c). This Cot CAR-T cell-selective cytotoxicity was also validated in human Cot CAR-T cells (hCot CAR-T cells; Supplementary Fig. 18). The small molecule toxins such as duocarmycin or emtansine conjugated with cotinine also showed similar selective cytotoxicity against Cot CAR-T cells (Supplementary Fig. 19).

Next, we evaluated whether Cot CAR-T cells could be depleted by Cot-saporin in vivo in an allogeneic CAR-T cell transfer model (Fig. 6d). When Balb/C mice transplanted with B6 bone marrow cells were injected with B6 Cot CAR-T cells, the transferred Cot CAR-T cells expanded in the peripheral blood in response to Balb/C alloantigen. However, when Cot-saporin was administered during this expansion phase, the Cot CAR-T cells failed to expand and were subsequently eliminated in the blood (Fig. 6e, f). Thus, Cot-saporin-mediated Cot CAR-T cell suicide was confirmed in vitro and in vivo.

https://doi.org/10.1038/s41467-024-53996-7

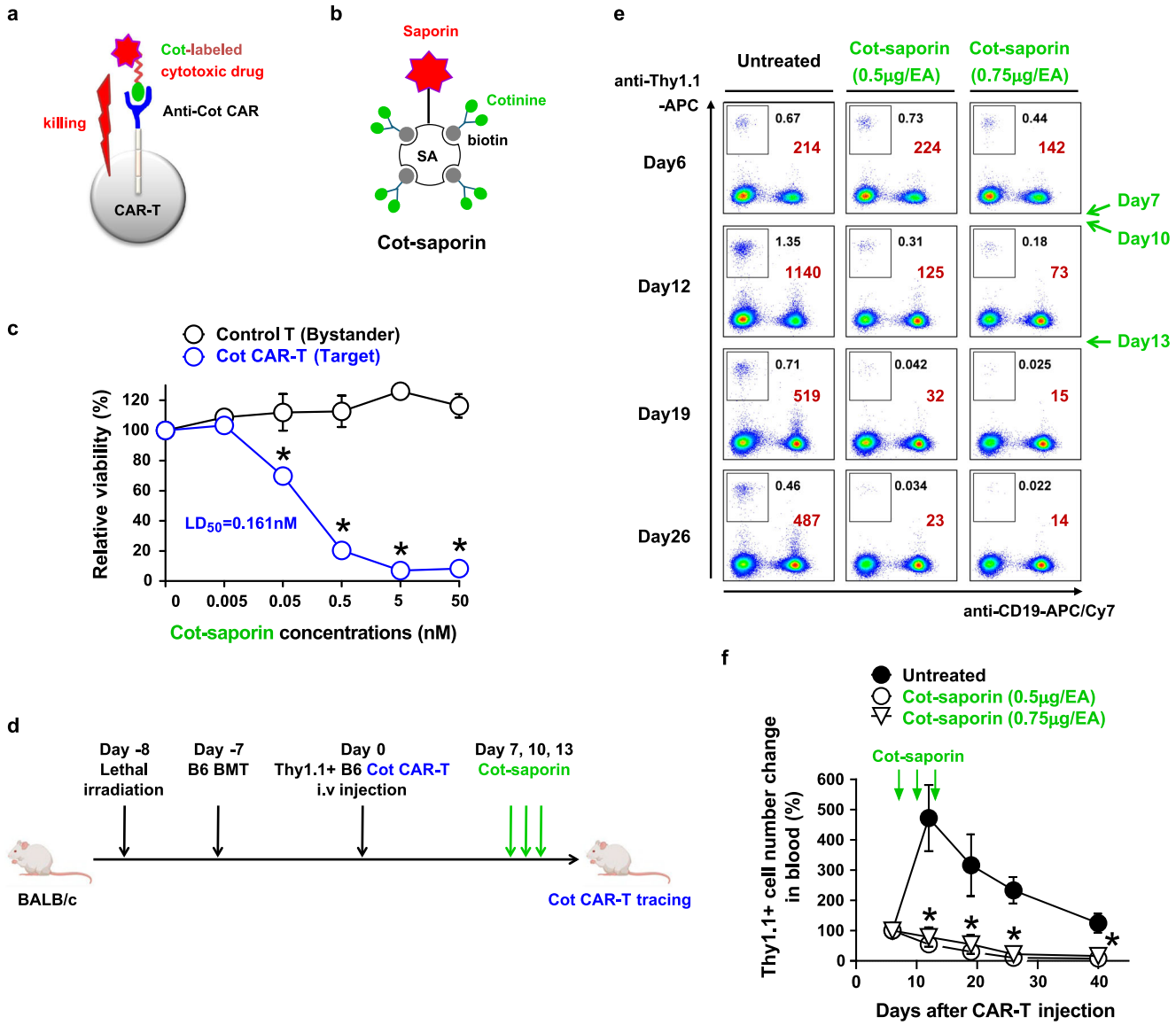

Fig. 6 | Anti-cotinine CAR can be used as a suicidal receptor using a cotinine-drug conjugate. a Scheme of Cot CAR-T cell suicide induced by a cotinine-labeled cytotoxic drug. **b** Schematic diagram of cotinine-labeled saporin (Cot-saporin). **c** In vitro toxicity of Cot-saporin on murine Cot CAR-T cells. Labeled control T cells (bystander) and unlabeled Cot CAR-T cells (target) were mixed in a 1:1 ratio and incubated with serial dilutions of Cot-saporin. After 48 h in a medium containing IL-2, viable bystander and target cells were counted, and viability was calculated as described in Methods. LD_{50} value is defined as the dose at which Cot-saporin was lethal for 50% of Cot CAR-T cells. Statistical significance was determined by unpaired two-tailed *t* test ($n = 3$, $p = 0.0059$ at 0.05 nM, $p = 0.0002$ at 0.5 nM, and $p < 0.0001$ at 5 nM and 50 nM). **d** Experimental scheme for in vivo depletion of allogeneic Cot CAR-T cells by Cot-saporin treatment. Lethally irradiated Balb/C mice were injected with T cell-depleted B6 BM cells. After 7 days, Cot CAR-T cells derived from Thy1.1-congenic B6 mice were sorted and injected *i.v.* into the mice. Cot-saporin (0.5 or 0.75 μg/head) was injected intraperitoneally three times at 3-day intervals from 7 days after CAR-T cell injection. **e** Cot CAR-T cells were traced by flow cytometry from 6 days after CAR-T cell transfer. Numbers are percentages (black) or absolute numbers (brown) of Cot CAR-T cells (boxes, $Thy1.1^+CD19^-$ cells) in a fixed volume (7 μl) of peripheral blood. **f** Relative kinetics of Cot CAR-T cell expansion in peripheral blood. Absolute numbers of Cot CAR-T cells at each time point in (**e**) were normalized to the numbers on day 6. Statistical significance between groups at each time point was determined by 1-way ANOVA ($n = 5$, *: $p = 0.0011$ on day 12, $p = 0.0122$ on day 19, $p < 0.0001$ on day 26, and $p = 0.0015$ on day 40, compared to the untreated group). Data in (**c** and **f**) are presented as mean ± SEM. Results are representative of two independent experiments (**c**, **e**, **f**). *p*: *p*-value. Source data are provided in the Source Data file.

Cotinine-drug conjugates alleviate allogeneic CAR-T cell-mediated delayed GVHD in recipients of allogeneic hematopoietic stem cell transplantation (allo-HSCT)

To evaluate the value of the suicidal adapter in a more clinically relevant setting, we modeled an allogeneic CAR-T cell-mediated GVHD side effect in mice (Fig. 7a). It has been reported in several preclinical and clinical studies that when hematological tumors relapse after allo-HSCT, CAR-T cells can be generated from the allogeneic donor and infused into the patients (recipients) to control the tumors[45–48]. The donor CAR-T cells are not rejected in the recipients due to HSCT-induced anti-donor immune tolerance and can show anti-tumor efficacy. However, they can induce GVHD by attacking recipient alloantigens even after tumor clearance[46–48]. Therefore, if late-phase GVHD develops, the donor CAR-T cells need to be physically eliminated to alleviate the GVHD. This GVHD toxicity cannot be controlled by simply removing the anti-tumor adapters, even for switchable CAR-T cells, because GVHD is induced by donor T cell recognition of recipient MHC through donor T cell receptor, not donor CAR.

Indeed, in a haploidentical allo-HSCT setting in which B6 donor bone marrow cells were transplanted into CB6F1 recipient mice (F1

https://doi.org/10.1038/s41467-024-53996-7

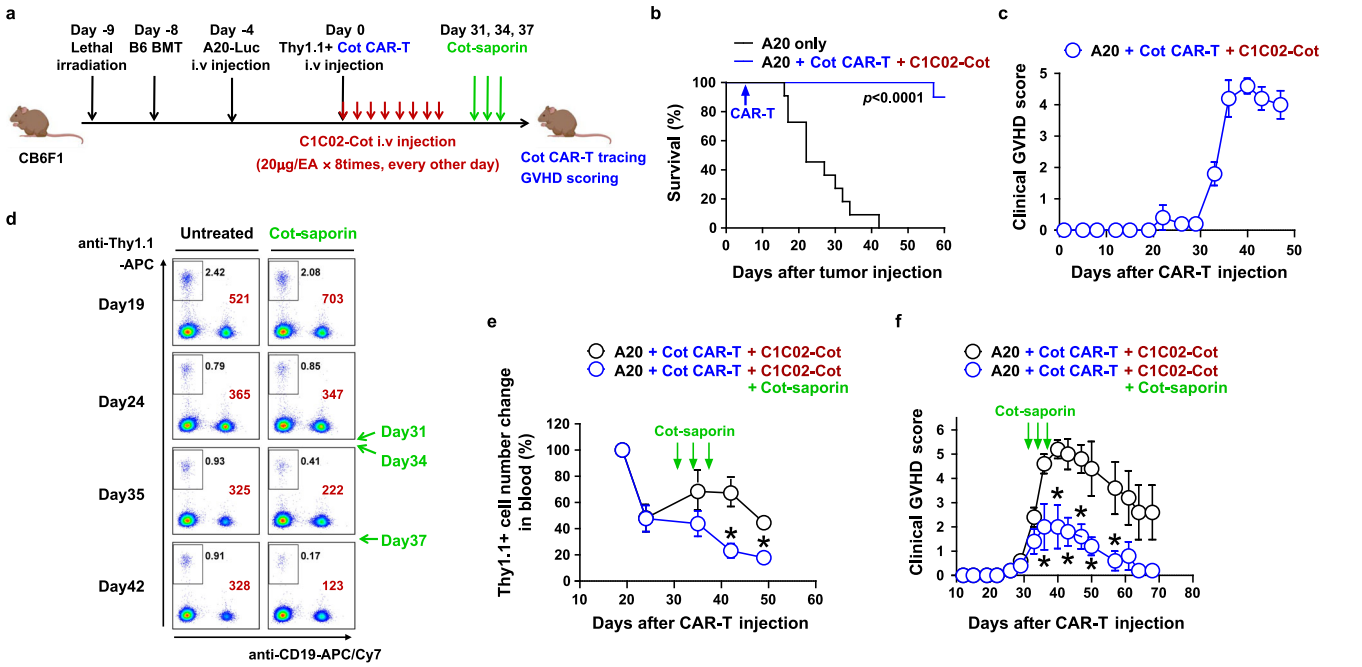

Fig. 7 | Cotinine-drug conjugate can eliminate allogeneic CAR-T cells after tumor eradication to reduce GVHD side effect. a Experimental scheme for alleviation of GVHD by Cot-Saporin in an allogeneic Cot CAR-T cell therapy model in haploidentical HSCT recipients. Lethally irradiated CB6F1 mice were injected with T cell-depleted B6 BM cells. After 4 days, A20-Luc cells were injected to mimic tumor recurrence after HSCT. Four days later, Cot CAR-T cells derived from Thy1.1-congenic B6 mice and C1C02-Cot proteins were administered as in Fig. 4a for tumor eradication. **b**, **c** Survival (**b**, $n = 10$) and clinical GVHD score (**c**, $n = 5$) were monitored periodically. Survival data were pooled from two replicate experiments. **d**–**f** The same experiment as in (**b**, **c**) was performed except that when GVHD began to develop after CAR-T cell injection, Cot-saporin (0.5 μg/head) was administered intraperitoneally three times at 3-day intervals (days 31, 34, and 37 after CAR-T cell injection). Cot CAR-T cells were traced by flow cytometry from 19 days after CAR-T cell transfer. Numbers are percentages (black) or absolute numbers (brown) of Cot CAR-T cells (boxes, $Thy1.1^+CD19^-$ cells) in a fixed volume (7 μl) of peripheral blood (**d**). Relative kinetics of Cot CAR-T cell expansion in peripheral blood (**e**). Absolute numbers of Cot CAR-T cells at each time point in (**d**) were normalized to the numbers on day 19 ($n = 5$). *: $p = 0.0053$ on day 42 and $p = 0.0015$ on day 49. Clinical GVHD score ($n = 5$) was monitored periodically (**f**). *: $p = 0.0355$ on day 36, $p = 0.0108$ on day 40, $p = 0.0059$ on day 43, $p = 0.0033$ on day 47, $p = 0.0269$ on day 50, and $p = 0.0311$ on day 57. Data in (**c**, **e**, **f**) are presented as mean ± SEM. Statistical significance was determined by log-rank (Mantel-Cox) test (**b**) or by unpaired two-tailed t test (**e**, **f**). Results are representative of at least two independent experiments (**b**–**f**). p: p-value. Source data are provided in the Source Data file.

mice from Balb/C and B6 cross-breeding), B6 donor Cot CAR-T cells injected with the CD40 adapter could efficiently control pre-implanted A20 Balb/C tumors, as shown by the improved survival of the recipient mice (Fig. 7a, b). However, the delayed severe GVHD developed one month after CAR-T cell transfer (Fig. 7c). Therefore, we administered Cot-saporin instead of a CD40 adapter after the onset of GVHD to eliminate Cot CAR-T cells. As expected, the number of Cot CAR-T cells in the peripheral blood decreased compared to the Cot-saporin-untreated group (Fig. 7d, e). Consistently, GVHD was significantly alleviated after Cot-saporin treatment (Fig. 7f). Cot-saporin treatment at this dose did not induce saporin-mediated toxicity, as body weight and survival of the mice were not affected by the treatment (Supplementary Fig. 20). In conclusion, the suicidal adapter could be a tool to eliminate unnecessary problematic switchable CAR-T cells after their beneficial use.

Discussion

The result of this study is one of the examples demonstrating that an optimal therapeutic window of a CAR-T cell can be established to maintain anti-tumor efficacy with minimal normal tissue toxicity with a single CAR system, obviating the need for dual CAR systems such as SynNotch, Split or iCARs. A representative single-CAR strategy to achieve this goal is "affinity-tuned CAR-T cells", in which the scFv in the CAR has a moderate affinity for the target antigen. Therefore, the CAR-T cells have sufficient reactivity to high-density antigens on tumor cells but do not respond to low-density antigens on normal tissues[49–51]. Although the concept is interesting, finding a good antibody that fits this "Goldilocks" affinity can be challenging, and the affinity of the scFv needs to be individually tuned to different targets. In this study, we show that the switchable CAR-T cells can achieve similar avidity tuning by adjusting the adapter doses. Interestingly, the in vitro efficacy of the switchable CAR-T cells was maintained at a dose 100-fold lower than the toxic dose, indicating a wide therapeutic window (Fig. 3i). The anti-CD40 scFv used in this study has a high affinity (nanomolar range), indicating that additional affinity tuning is not necessary for the switchable CAR system (Supplementary Fig. 1). Similar avidity tuning by small molecule drugs has also been proposed. In this strategy, the CAR molecule has degradable domains or protease-sensitive domains, allowing the expression level or activity of CARs to be regulated by degradation inducers or protease inhibitors[52–55]. Recently, it has been directly demonstrated that avidity tuning of these drug-regulatable CARs by adjusting drug doses can mitigate on-target off-tumor toxicity while maintaining anti-tumor efficacy[55]. Thus, the concept of avidity tuning of CAR-T cells may be a general principle to solve the problem of on-target off-tumor toxicity.

Besides the avidity tuning effect, the switchable CAR system may have additional kinetic and spatial advantages in vivo. The scFv or Fab adapters have a short serum half-life, typically within a few hours[56–58], and therefore need to be infused frequently. Although this short half-life has been highlighted by the rapid turning-off of acute CAR toxicity by stopping the infusion, regular infusion of the short-acting adapters may also lead to intermittent turning-off of excessive CAR-T cell activation in vivo. In contrast, the adapters are known to reside much longer at the tumor site than in the blood[56], which may lead to stronger activation of CAR-T cells recruited to the inflamed tumor site. In addition, intermittent long-term rest (1 to 2 weeks) of adapter infusion

may prevent CAR-T cell exhaustion and further enhance CAR-T cell efficacy in vivo, as reported[38]. The switchable CAR-T system, targeting a single antigen, also has its shortcomings. Tumors with relatively low tumor antigen levels, tumors with down-regulated tumor antigens, or tumors with antigenic heterogeneity may not be efficiently eliminated by switchable CAR-T cells. In these cases, multi-antigen targeting by adding adapters against a second or third tumor antigen, as originally proposed, may be useful[17,18]. However, the practical hurdle would be that the adapters would have to be produced as a separate protein drug for each individual target, increasing the cost of the overall treatment. Nonetheless, in the long run, once the number of adapters produced has accumulated, multi-antigen targeting with one CAR-T cell product and personalized selection of adapters depending on antigen expression in the individual patient would be advantageous.

Although the high expression of CD40 in tumors and the stimulatory role of CD40 in dendritic cells and macrophages have led to the extensive development of both antagonistic and agonistic antibodies, the therapeutic efficacy of anti-CD40 antibodies in clinical trials has not been very impressive[59]. Therefore, CD40 may be a target for CAR-T cell development to improve the efficacy of the antagonistic strategy. However, although anti-CD40 antibodies are relatively safe at current doses in clinical trials[26], higher doses of anti-CD40 antibodies may be potentially toxic due to hyperactivation of immune cells or effects on CD40-expressing parenchymal cells[29,59,60]. These concerns may have prevented the emergence of CD40 as a CAR target in the research community. In this study, we confirmed that these concerns are valid in the mode of conventional CAR-T cell therapy. Particularly, CAR-T cell accumulation accompanied by severe acute perivasculitis in the lung preceded acute lethality in CD40 CAR-T cell-treated mice. CD40 has been reported to be expressed in murine lung endothelium[61,62]. A high expression of CD40 mRNA in vascular cells compared to other cell types in the lung could also be identified using a recently published single-cell RNA sequencing database of mouse and human lungs[63] (Supplementary Fig. 9). However, at the protein level, CD40 expression on lung endothelium could only be detected by highly sensitive radiolabeled anti-CD40 antibodies and not by conventional immunohistochemical staining, suggesting that the surface expression level of CD40 on lung endothelium is very low[61,62]. Nevertheless, CD40 CAR-T cells seemed to recognize this low level of CD40 in lung endothelium and induce severe inflammation. It is well known that pulmonary endothelial damage can lead to acute lung injury with high mortality[64]. In contrast, the switchable CAR T cells did not accumulate in the lung or induce lung inflammation, suggesting that these CAR T cells ignored the low level of CD40 in the lung endothelium and concentrated on CD40-high tumor cells, consistent with the avidity tuning effect proposed in this study. Coherently, switchable CAR T cells showed much lower cytotoxicity on other CD40-low cells, such as macrophages and dendritic cells. Furthermore, they also showed a partial stimulatory effect on dendritic cells, similar to previously published CD40L-expressing CAR T cells[65] (Supplementary Fig. 12). Thus, the switchable CAR system alleviated toxicity concerns about CD40 and demonstrated that CD40 can be an attractive target for CAR-T cell therapy.

The epitope tag for the switchable adapter should be carefully selected. It needs to be biologically inert and non-toxic. In this sense, cotinine seems to be one of the appropriate chemical tags for the adapters. As a nicotine metabolite, it has been shown to be safe for smokers, although there is some debate about its mild neuroprotective or neuropsychiatric role[66,67]. The other problem with chemical tags would be the difficulty in maintaining a consistent molar ratio of adapter and conjugated chemical (DAR). In this study, we proved that the introduction of a cysteine residue into the framework region of the antibody adapter can be successfully used for equimolar conjugation of cotinine (DAR 1). Other strategies, such as genetic peptide epitope tagging to the scFv adapters, would be an alternative option, as validated in a recent clinical trial[58].

Finally, the cytotoxic drug-labeled tag for the physical removal of CAR-T cells could be the ultimate option for long-term safety. The advantage of this tag-drug conjugate would be that no additional suicidal genetic modification of the CAR-T cells would be required. Simply replacing the tumor-targeting adapter with the cotinine-drug conjugate would be sufficient to selectively eliminate CAR-T cells. The disadvantage of this strategy compared to others using clinically approved anti-CD20 or anti-EGFR antibodies would be that these reagents would have to be newly manufactured and clinically tested. Nonetheless, many cytotoxic drugs have been developed for similar purposes for antibody-drug conjugates[68], and unlike biologically produced antibody drugs, cotinine-drug conjugates can be chemically synthesized or conjugated. Thus, the development of these drugs is relatively feasible.

In conclusion, we have shown that the switchable CAR-T cells are a valid option for untargetable tumor antigens due to on-target off-tumor toxicity and that anti-CD40 switchable CAR-T cells can be effective therapeutics for the treatment of hematological malignancies. In addition, the cytotoxic drug-labeled tag can provide a last tool to guarantee the safety of switchable CAR-T cells.

Methods

Mice

Balb/C and C57BL/6 (B6) mice were purchased from Orient Bio (Korea). Thy1.1 congenic (000406; B6.PL-Thy1^{a}/CyJ), CD40 knockout (002928; B6.129P2-Cd40^{tm1Kik}/J), and albino (000058; B6(Cg)-Tyrc-2J/J) mice on a B6 background, and NSG (005557; NOD.Cg-Prkdc^{scid} Il2rg^{tm1Wjl}/SzJ) mice were from The Jackson Laboratory (USA). CB6F1 mice were from Japan SLC. All mice were housed in a specific pathogen-free animal facility at the Seoul National University College of Medicine and maintained in accordance with the guidelines of the Institutional Animal Care and Use Committee (IACUC). The experimental use of animals was approved by the IACUC (SNU-160602-17, SNU-200713-4). Experimental and control group mice were housed separately in individually ventilated cage racks in the same room. Euthanasia was performed by CO_2 inhalation.

Cell lines

A20 (TIB-208; B cell lymphoma on a Balb/C background), EL4 (TIB-39; lymphoma on a B6 background), Raji (CCL-86; human B cell lymphoma), AU565 (CRL-2351; human mammary gland adenocarcinoma), and PG-13 (CRL-3597; retroviral packaging cell line) were purchased from the American Type Culture Collection (ATCC, USA). Daudi (10213; human B cell lymphoma) cells were from the Korean Cell Line Bank. Phoenix GP and Phoenix Eco cell lines were provided by Garry Nolan (Stanford University, USA). To generate the mouse CD40-expressing EL4 cell line (EL4-mCD40), mouse CD40 was cloned into a pMP vector from pCMV6-Entry-mCD40 (MR227111; OriGene, USA), then retrovirus was generated and spin-infected into EL4. CD40-deleted A20 cell line was generated by electroporation-based CRISPR/Cas9 delivery method using Cas9 protein and mouse CD40 targeting sgRNA (Mm.Cas9.CD40.1.AB; TCAAGGGCTTCGGGTTAAGAAGG; IDT, USA).

Luciferase-GFP-expressing tumor cell lines (A20-Luc, CD40-deleted A20-Luc, EL4-mCD40-Luc, and Daudi-Luc) were generated by spin infection with a retrovirus (pMP-LucGFP) or lentivirus (pLEF-LucGFP) harboring the luciferase-P2A-EGFP expression cassette. GFP-high populations were sorted with a FACS Aria II Cell Sorter (Becton Dickinson, USA).

Generation of antibodies to mouse or human CD40 proteins

White leghorn chickens were immunized four times with recombinant mouse CD40 protein (50324-M08H; Sino Biological, China) or human CD40 protein (10774-H08H; Sino Biological). Total RNA from the bursa of Fabricius, spleen, and bone marrow was isolated with TRIzol reagent (Invitrogen, USA), and cDNA was synthesized with a SuperScript III First-Strand cDNA Synthesis Kit with oligo (dT) primers (Invitrogen)

according to the manufacturer's instructions. scFv phage-display libraries were constructed from the cDNAs as described previously[69]. Four rounds of bio-panning were performed against mouse or human CD40 protein coated on paramagnetic Dynabeads (Invitrogen). The scFv clones were selected via phage ELISA against mouse or human CD40 protein using horseradish peroxidase (HRP)-conjugated anti-M13 antibody (11973-MM05; Sino Biological). Recombinant scFv proteins fused to the constant region of human immunoglobulin kappa light chain (scFv-Cκ) were produced from Expi293F cells (A14527; Invitrogen) and purified by anti-Cκ affinity chromatography (KappaSelect, 17545811; Cytiva, USA). The specific binding of scFv-Cκ proteins to CD40 proteins was validated via ELISA. Briefly, serial diluents of anti-CD40 scFv-Cκ or irrelevant scFv -Cκ proteins were loaded into the wells of the 96-well plates coated with mouse CD40-Fc (1215-CD; R&D Systems, USA) or human CD40-Fc (1493-CDB; R&D Systems) proteins. The binding of the scFv-Cκs was measured with a secondary antibody (anti-human Cκ-HRP; AP502P; Sigma-Aldrich, USA).

Preparation of cotinine-labeled adapters

For random conjugation of cotinine with full-length immunoglobulins such as rituximab (Mabthera; Roche) and trastuzumab (Herceptin; Roche), EDC coupling was used. Trans-4-cotinine-carboxylic acid (347574; Sigma-Aldrich), 1-ethyl-3-(3-dimethylaminopropyl) carbodiimide (77149; Thermo Scientific, USA), and N-hydroxysulfosuccinimide (24500; Thermo Scientific) were mixed at a 1:10:25 molar ratio for 15 min to form NHS esters with cotinine. Then two-hundred molar excess of activated NHS-ester solution was incubated with the antibody solution for 3 h at room temperature. The conjugated antibodies were retrieved by dialysis in phosphate-buffered saline (PBS) and used for experiments. For site-specific conjugation of cotinine with scFv-Cκ proteins, an artificial cysteine residue was introduced at position 13 (Kabat numbering) of the framework of heavy chain variable region (V_H T13C)[37]. The variant scFv-Cκ proteins were incubated with 100 equivalents of Tris (2-carboxyethyl) phosphine (TCEP) in PBS with 25 mM EDTA at 37 °C for 18 h. To remove excess TCEP, the mixture was subjected to size-exclusion chromatography (Zeba™ spin desalting columns, 7 K cut-off; Thermo Scientific). Next, for the maleimide-thiol alkylation reaction, the reduced scFv-Cκ proteins were incubated with 100 equivalents of maleimide-PEG_8-cotinine in PBS with 25 mM EDTA at 25 °C for 18 h. The cotinine-conjugated scFv-Cκs were purified by size-exclusion chromatography for further use. Cell-surface binding of the cotinine-conjugated antibodies was detected with an anti-cotinine antibody labeled in-house with APC (LNK032APC; Bio-Rad Laboratories) or an anti-Kappa antibody labeled with APC (341108; BD Biosciences, USA) by flow cytometry.

Preparation of the CAR construct

The anti-CD40 murine CAR ORF consists of a mouse Ig kappa leader, anti-mouse CD40 scFv (clone C1C02), and a mouse CD28-based CAR backbone reported previously (mouse CD28 extracellular and transmembrane domains linked to the mouse CD3zeta cytoplasmic domain, [GenBank HM754222.1])[70]. The leader and scFv portions were amplified by PCR and linked to the synthesized CAR backbone DNA (Bioneer, Korea) by blunt-end ligation. The CAR ORF was cloned into the downstream region of the PGK promoter, replacing the PuroR gene, of the pMSCV-puro retroviral vector (Clontech, USA; pMP-CD40-Rm28z) for murine CAR-T cell production. The anti-cotinine murine CAR retroviral vector (pMP-Cot-Rm28z) was constructed in a similar way with an anti-cotinine scFv generated previously[71]. For in vivo tracing of CAR-T cells, retroviral vectors encoding both CAR and enhanced firefly luciferase (efflux) ORFs simultaneously were generated. PCR-amplified Cot-Rm28z or CD40-Rm28z ORF was blunt-end ligated with T2A-efflux ORF amplified from pDONR222-eGFP-effLuc (a gift from Dr. Rabinovsky, MD Anderson Cancer Center, USA) and cloned into pMSCV-puro as described above (pMP-CD40-Rm28z-T2A-effluc, pMP-Cot-Rm28z-T2A-effluc). For the control effluc plasmid, the GFP ORF from pEGFP-C1 (Clontech) and T2A-effluc ORF were ligated and cloned into pMSCV-puro (pMP-GFP-T2A-effluc). The anti-cotinine human CAR ORF consists of a human GM-CSFR leader, human codon-optimized anti-cotinine scFv, and a human CD28-based CAR backbone (human CD28 extracellular and transmembrane domains linked to the human CD3zeta cytoplasmic domain [GenBank HM852952.1])[72]. CAR ORF DNA was synthesized (GeneArt, Germany; Integrated DNA Technologies, USA) and cloned into the pMSGV retroviral vector (Addgene plasmid #64269; pMSGV-hCot-28z) for the production of human CAR-T cells.

Preparation of CAR retroviruses

To produce ecotropic retroviruses for mouse T cell transduction, the CAR retroviral plasmid was transfected into the Phoenix GP cells together with the VSV-G envelop expression plasmid (pMD2.G, Addgene plasmid #12259) using Lipofectamine 3000 (Invitrogen). After 48 h, the culture supernatant containing the VSV-G-pseudotyped retrovirus was harvested and incubated with a Phoenix Eco cell line to stably transduce the retroviral cDNA. Three to five days after infection, the transduced Phoenix Eco cells expressing CAR on the surface were sorted to establish retrovirus-producing cell lines (FACS Aria II, Becton Dickinson, USA). The retroviral culture supernatant produced from this cell line was concentrated 5- to 10-fold with a centrifugal filter device (Amicon Ultra-100 kDa cut-off; Millipore, USA) for further use. To obtain an amphotropic retrovirus for human T cell transduction, the CAR retroviral plasmid for human T cells was transfected into the Phoenix Eco cell line using Lipofectamine 3000. After 48 h, the culture supernatant was harvested and incubated with PG13 cells (derived from mouse fibroblasts) for stable transduction of the retroviral cDNA. The retrovirus-producing cell line was established by cell sorting based on CAR expression, and the retrovirus was produced and concentrated similarly to the murine virus-producing cell lines.

Generation of CAR-T cells

For CAR retroviral transduction of mouse T cells, spleen, and lymph node cells were stimulated with plate-bound anti-CD3 (10 μg/ml; 145-2C11; BioXCell, USA) and anti-CD28 (2 μg/ml; 37.51; BD Biosciences) antibodies. The next day, retrovirus particles were attached to retronectin-coated plates by centrifugation at 2000 × *g* for 2 h, and activated T cells were added and transduced by centrifugation at 1000 × *g* for 10 min. After 2 days, the transduced T cells were transferred to a fresh medium containing 200 μ/ml recombinant human IL-2 (Proleukin, Novartis, Switzerland) and expanded for 2 to 3 days without further stimulation. The transduction efficiency of CAR-T cells was estimated by surface CAR staining with a fluorescein isothiocyanate (FITC)-conjugated Fab against rabbit IgG (Jackson ImmunoResearch, USA) for Cot-CAR or a FITC-conjugated Fab against chicken IgY (LSBio, Seattle, USA) for CD40-CAR and analyzed by flow cytometry using FlowJo software (TreeStar, Inc., USA).

For human CAR-T cells, human peripheral blood was obtained from healthy volunteers who provided written informed consent according to a protocol approved by the Institutional Review Board of Seoul National University Hospital (IRB No. 1805-153-948). PBMCs prepared by Ficoll-gradient centrifugation (841 × *g*, 20 min, RT) were stimulated with plate-bound anti-CD3 (10 μg/ml; OKT3; BioXCell) and anti-CD28 (2 μg/ml; CD28.2; BD Biosciences) antibodies. After 2 days, activated human T cells were transduced similarly to mouse T cells. After 2 days, the transduced T cells were transferred to a fresh medium containing 200 μ/ml recombinant human IL-2 and expanded for 3 days without further stimulation. For in vivo experiments, human CAR-T cells were expanded in fresh medium containing 200 μ/ml human IL-2 for an additional 3 days. The transduction efficiency of human Cot CAR-T cells was also measured by CAR staining as for mouse Cot CAR-T cells. Control T cells were generated using the same protocol as for CAR-T cell generation except for retroviral transduction.

In vitro functional activity of CAR-T cells

For cytotoxicity assay, target tumor cells were labeled with PKH26 (Sigma-Aldrich) according to the manufacturer's instructions. Tumor cells (target; 5×10^4) and CAR-T cells (effector) were mixed at various effector: target (E:T) ratios (0:1 to 25:1) in 500 µl culture medium per reaction and incubated for 6 h, followed by 7-AAD staining (Biolegend, USA). The number of viable tumor cells (7-AAD$^-$, PKH$^+$) was determined with the cell-counting beads (123count eBeads; Thermo Fisher Scientific) by flow cytometry. Percent cytotoxicity was calculated as follows: (number of viable tumor cells in the tube without CAR-T cells - number of viable tumor cells in the tube with CAR-T cells) / number of viable tumor cells in the tube without CAR-T cells × 100. To evaluate CAR-T cell activation, CAR-T cells (2×10^4) were co-cultured with target tumor cells (1×10^5) for 24 h. The culture supernatants were harvested, and the amounts of IFN-γ produced were measured using a mouse or human IFN-γ ELISA set (BD Bioscience) according to the manufacturer's instructions. For Cot CAR-T cells, PKH-stained target cells were preincubated with a cotinine-labeled adapter for 1 h and washed to remove the free adapter prior to incubation with CAR-T cells for both cytotoxicity and cytokine production assays.

Cytokine production by macrophages and dendritic cells

To isolate macrophages, Balb/C mice were injected intraperitoneally with 1 ml 3% Brewer thioglycollate medium (Difco, USA). After 5–7 days, peritoneal lavage fluid was harvested with 10 ml RPMI-1640 medium with 2.5% FBS, and macrophages were purified using a macrophage isolation kit (Milteny Biotec, Germany). Approximately 70% of the cells were F4/80-positive. To isolate dendritic cells (DCs), spleens of Balb/C mice were dissected and treated with collagenase D. After Nycodenz (Sigma-Aldrich) gradient centrifugation, DCs were purified using Pan DC microbeads (Milteny Biotec). Approximately 75% of the cells were CD11c-positive. Macrophages or DCs (5×10^4) were co-cultured with CAR-T cells (1×10^4) for 24 h, and the supernatants were harvested to measure the amounts of IL-6 (Biolegend), IL-12 (BD Bioscience), and IL-1β (Thermo Fisher Scientific) by ELISA according to the manufacturer's instructions. For Cot CAR-T cells, macrophages or DCs were preincubated with a cotinine-labeled adapter for 1 h and washed to remove the free adapter prior to incubation with CAR-T cells. Cytotoxicity of macrophages and DCs by CAR-T cells was tested in the same manner as antitumor cytotoxicity above.

In vivo CAR-T cell therapy models

For syngeneic murine CAR-T cell therapy models, Balb/C mice (female, 6–8 weeks) were inoculated intravenously with A20-Luc cells (1×10^6). After 6 days, the mice were irradiated (2.5 Gy) for lymphodepletion. The next day, CD40 CAR-T or Cot CAR-T cells (5×10^6) were administered intravenously. For Cot CAR-T cells, the cotinine-labeled adapter (C1C02-Cot; 20 µg) was injected intravenously, once every other day, beginning on the day of CAR-T cell administration, for a total of eight times. For murine CAR-T cell therapy in CD40 knockout B6 mice, wild type B6 or CD40 knockout B6 (female and male, 8 weeks) mice were intravenously inoculated with EL4-mCD40-Luc (5×10^5), and B6 CAR-T cell treatment was performed as in Balb/C, except for 3 Gy irradiation for lymphodepletion. For a xenogeneic human CAR-T cell therapy model, NSG mice (female and male, 6–8 weeks) were inoculated with Daudi-Luc cells (5×10^5) intravenously. Three days later, hCot CAR-T cells (1×10^7) were administered intravenously. The cotinine-labeled anti-human CD40 adapter (2B1-Cot, 25 µg) was injected intravenously every other day from the day of CAR-T cell administration, for a total of eight times. To evaluate therapeutic efficacy, tumor burden was measured by weekly peritoneal injection of D-luciferin (2 mg/head; Promega, USA) and bioluminescence imaging using IVIS 100 (PerkinElmer, USA) or Lumina S5 (GE, USA).

For cytokine neutralization experiments, anti-mIL-6 (MP5-20F3; BioXCell) and/or anti-mIL-12 p40 (C17.8; BioXCell) was administered intraperitoneally once a day for six consecutive days beginning 5 h before CAR-T cell transfer (Use 500 µg of anti-mIL-6 and/or anti-mIL-12 for the first dose, followed by 250 µg of anti-mIL-6 and/or 500 µg of anti-mIL-12 for the next 5 days). Anakinra (Kineret; Swedish Orphan Biovitrum, Sweden) was administered intraperitoneally at a dose of 600 µg once a day for 5 days, beginning 5 h before CAR-T cell transfer[32]. For macrophage depletion, mice were treated intraperitoneally with clodronate liposome (1 mg; Liposoma, The Netherlands) for three consecutive days prior to CAR-T cell infusion[31].

For in vivo CAR-T cell tracing, Balb/C T cells expressing both CAR and effluc (CAR-Luc-T cells) or control T cells expressing both GFP and effluc (Control-Luc-T cells) (1×10^6 or 5×10^6) were transferred intravenously to irradiated (2.5 Gy) Balb/C mice. CAR-T cell trafficking was monitored by bioluminescence imaging 6 h, 1, 3, and 7 days after CAR-T cell injection. In some experiments, A20 cells (2×10^7) were injected subcutaneously 13 days before CAR-T cell transfer.

Generation of bone marrow chimera mice

Recipient wild-type or CD40 knockout mice (female, 6 weeks) on B6 background were lethally irradiated (total 7.5 Gy divided into 4 Gy plus 3.5 Gy, separated by 4 h). The next day, the mice were intravenously injected with $5\text{-}6 \times 10^6$ T cell-depleted donor (B6 or CD40 knockout) bone marrow (BM) cells. In detail, BM cells were isolated from the tibia and femur of mice, and T cells were depleted with a cocktail of anti-Thy1.2 (30-H12), anti-CD4 (GK1.5), and anti-CD8 (53–6.7) antibodies (BD Biosciences) and guinea pig complement (Cedarlane, Canada) as previously described[73]. Chimerism in peripheral blood was assessed 5–7 weeks after BM transplantation (BMT) by flow cytometry. FITC-conjugated anti-mCD40 (3/23; BD Biosciences) was used to check the establishment of donor chimerism in the recipient's peripheral blood. Eight weeks after BMT, CD40 CAR-T cells generated from B6 lymphocytes were transferred to the recipients. Mouse survival and body weight changes were monitored regularly.

In vitro Cot CAR-T cell depletion by cotinine-drug conjugates

Bivalent cotinine- and monovalent biotin-conjugated hexapeptide (Cotinine-Gly-Ser-Lys[Biotin]-Gly-Ser-Lys-Cotinine) were chemically synthesized by Peptron (Korea). The peptides were incubated with saporin-labeled streptavidin (Advanced Targeting Systems, USA) at a molar ratio of 4:1 to generate cotinine-saporin conjugate (Cot-saporin)[42]. For Cot-saporin-dependent cytotoxicity assays on Cot CAR-T cells, a 1:1 mixed population (50,000 cells each) of Cot CAR-T cells (target cells) and control T cells (bystander non-CAR-T cells) were incubated with various doses of Cot-saporin for 48 h in medium containing human IL-2 (500U/ml). Control T cells were generated using the Cot CAR-T cell generation protocol except for retroviral transduction. To differentiate the two populations, control T cells were prelabeled with PKH26 dye, and Cot CAR-T cells were stained with anti-CAR antibody (FITC-labeled anti-rabbit IgG Fab) at the end of the culture. Cells were stained with 7-AAD at the end of the culture to exclude dead cells. The number of viable target (7-AAD$^-$, Cot-CAR$^+$) or control (7-AAD$^-$, PKH26$^+$) T cells after incubation was determined by flow cytometry using cell-counting beads. Percent viability was calculated as follows: number of viable cells in the tube with the drug / number of viable cells in the tube without the drug × 100. LD_{50} values were calculated using SigmaPlot software (Systat Software, USA). Cotinine drug conjugates using small molecule toxins (duocarmycin or emtansine (DM−1)) were also synthesized (Concortis Biosystems Corp. USA) and tested in the same manner as above. These include Cot-duocarmycin (trans-4-Cot-PEG4-vc-PAB-ducoramycin SA), 2 × Cot-4 × duocarmycin ([Cot-GSKGSKGSKGSKK-Cot](PEG-vc-PAB-DMAE-duocarmycin SA)$_4$) and 2 × Cot-4 × -DM1 ([Cot-GSKGSKGSKGSKK-Cot](Lys-MCC-DM1)$_4$).

In vivo Cot CAR-T cell depletion

For the allogeneic CAR-T cell transfer model, Balb/C mice (female, 6 weeks) were lethally irradiated (total 5.5 Gy divided into 3 Gy plus 2.5 Gy, separated by 4 h) and T cell-depleted B6 BM cells were transferred the next day as described above. Cot CAR-T cells were generated from lymphocytes of Thy1.1 congenic B6 mice. Seven days after BMT, Thy1.1$^+$ Cot CAR$^+$ T cells were purified by cell sorting and injected intravenously into recipient Balb/C mice. Seven days after CAR-T cell transfer, Cot-saporin was administered intraperitoneally three times at 3-day intervals. The number of viable CAR-T cells (CD19$^-$, Thy1.1$^+$, 7-AAD$^-$) in the peripheral blood was determined by flow cytometry using cell-counting beads.

For the allogeneic CAR-T cell therapy model in the haploidentical allo-HSCT setting, B6 bone marrow cells were administered to lethally irradiated (total 7.5 Gy split) CB6F1 mice (female, 6 weeks, offspring of Balb/C and B6 mice cross-breeding) as described above. Four days after BMT, A20 cells were intravenously inoculated into recipient CB6F1 mice. After 4 days, Cot CAR-T cells were generated from Thy1.1 congenic B6 mice and injected intravenously along with C1C02-Cot (20 μg/head) 8 times every other day. Thirty-one days after CAR-T cell transfer, Cot-saporin administration and measurement of viable CAR-T cells in peripheral blood were performed as above. Body weight was measured regularly. The severity of GVHD was assessed twice weekly by measuring changes in the skin (alopecia, inflamed or scaly skin), generalized signs (fur texture, posture, and activity), eye inflammation, and diarrhea. Each parameter was quantified using the following scoring system: 0, normal; 1, mild; 2, moderate; and 3, severe (for eye inflammation, 4 indicated that both eyes were severely inflamed and closed). The total clinical GVHD score was defined as the sum of the scores for each parameter[74].

Histological analysis of mouse tissues

Balb/C mice were anesthetized and perfused transcardially with 10 ml PBS. Various organs (lung, liver, spleen, intestine, and kidney) were isolated, fixed in 4% paraformaldehyde in PBS, and embedded in paraffin. Paraffin sections were stained with hematoxylin and eosin (H&E) for histological examination. For immunohistochemical staining for CD40, 4 μm paraffin sections were deparaffinized and rehydrated before staining. Endogenous peroxidase activity was blocked with 3% hydrogen peroxide in methanol for 10 min. Slides were then blocked with 1% bovine serum albumin in PBS for 1 h and stained with C1C02-Cκ as primary antibody at 4 °C for 24 h. CD40 expression was detected by secondary antibody staining with biotinylated goat anti-human kappa light chain (Invitrogen) and third antibody staining with avidin-HRP (Biolegend), followed by chromogenic reaction using a DAB substrate kit (DAB057; Zytomed, Germany). The slides were counterstained with hematoxylin (Sigma-Aldrich).

qRT-PCR

Perfused and dissected Balb/C mouse organs (lung, liver, spleen, intestine, and kidney) were homogenized using a TissueLyser II (Qiagen, Germany), and total RNA was extracted using TRIzol reagent (Invitrogen). cDNA was generated using PrimeScript™ RT Reagent (Takara Bio, Japan). qRT-PCR was performed using KAPA SYBR FAST qPCR Master Mix (KAPA Biosystems, USA) in triplicate. The level of CD40 mRNA was normalized to that of β-actin mRNA. Primer sequences were as follows: for mouse CD40, forward: 5′-CTGTGAACCCAATCAAGGGC-3′ and reverse: 5′-GACGGTATCAGTGGTCTCAG-3′; for mouse β-actin, forward: 5′-CGTGAAAAGATGACCCAGATCA-3′ and reverse: 5′-TGGTACGACCA GAGGCATACA-3′.

Flow cytometry

Cells were washed with FACS buffer (0.2% BSA, 0.1% sodium azide, and 2 mM EDTA in PBS) and then stained with fluorescence-labeled antibodies in the dark for 25 min at 4 °C. TruStain FcX™ PLUS (anti-mCD16/32) (Biolegend, #156604, 2 μl/sample) was used prior to staining mouse single cell suspensions. CD40 CAR expression on mouse T cells was detected with goat anti-chicken IgY-FITC (IgG Fab polyclonal, LSBio, #LS-C61573, 1:200 dilution). AffiniPure Fab fragment goat anti-rabbit IgG (H + L)-FITC (IgG Fab polyclonal, Jackson ImmunoResearch, #111-097-003, 1:200 dilution) was used to detect Cot CAR expression on human and mouse T cells. Anti-cotinine antibody was conjugated in-house using the Rapid APC Antibody Conjugation Kit (LNK032APC, Bio-rad Laboratories) and used to detect cotinine-tagged adapters binding to cells (1:500 dilution). The following antibodies were used to stain cell surface molecules. Anti-mCD40-FITC (3/23, BD Biosciences, #561845, 1:200 dilution), Rat IgG2a, κ Isotype Ctr-FITC (R35-95, BD Biosciences, #553929, 1:200 dilution), anti-mCD86-FITC (GL1, BD Pharmingen, #553691, 1:200 dilution), anti-mCD40-PE (3/23, BD Biosciences, #553791, 1:500 dilution), Rat IgG2a, κ Isotype Ctr-PE (R35-95, BD Biosciences, #553930, 1:500 dilution), anti-mCD4-PE (RM4-4, Biolegend, #116006, 1:1000 dilution), anti-mCD8a-PerCP/Cy5.5 (53-6.7; Biolegend, #100722, 1:300 dilution), anti-Thy1.2(CD90.2)-APC (53-2.1, Biolegend, #140312, 1:500 dilution), anti-Thy1.1(CD90.1)-APC (OX-7, Biolegend, #202526, 1:500 dilution), anti-mCD19-APC/Cy7 (6D5, Biolegend, #115529, 1:300 dilution), anti-mCD4-APC/Cy7 (GK1.5, Biolegend, #100414, 1:300 dilution), anti-mCD3-BV421 (17A2, Biolegend, #100218, 1:500 dilution), anti-mCD11b-FITC (M1/70, Biolegend, #101205, 1:200 dilution), anti-mF4/80-PE (BM8, Biolegend, #123109, 1:500 dilution), anti-mCD11c-PE (N418, Biolegend, #117307, 1:500 dilution), anti-hCD4-FITC (RPA-T4, Biolegend, #300506, 1:100 dilution), anti-hCD40-PE (5C3, Biolegend, #334308, 1:100 dilution), Mouse IgG1, κ Isotype Ctrl-PE (MOPC-21, Biolegend, #400111, 1:100 dilution), anti-hCD8a-PerCP/Cy5.5 (HIT8a, Biolegend, #300924, 1:100 dilution), anti-hCD4-PE/Cy7 (RPA-T4, Biolegend, #300512, 1:100 dilution), anti-human kappa light chain-APC (TB28-2, BD Biosciences, #341108, 1:100 dilution), anti-hCD4-APC/Cy7 (SK3, Biolegend, #344616, 1:100 dilution), anti-hCD45-BV421 (HI30, Biolegend, #304032, 1:100 dilution), anti-hCD4-BV510 (RPA-T4, Biolegend, #300546, 1:100 dilution), anti-mCD80-BV421 (16-10A1, Biolegend, #104725, 1:500 dilution), anti-mH-2K^b-APC (AF6-88.5, Biolegend, #116517, 1:500 dilution), anti-mH-2K^d-APC (SF1-1.1, Biolegend, #116619, 1:500 dilution), and Streptavidin-PE (Biolegend, #554061, 1:1000 dilution). Dead cells were excluded using 7-AAD Viability Staining Solution (Biolegend, #420404, 5 μl/sample), and 123count eBeads (Invitrogen, #01-1234-42, 10 μl/sample) were used to obtain absolute cell counts in each sample tube. All data were collected using BD FACSCanto II or BD FACSLyric cytometer (BD Biosciences) equipped with the FACSDiva software (BD Biosciences) and analyzed using FlowJo version 10 software (BD Biosciences).

Statistical analysis

Statistical analysis between two groups was performed using an unpaired two-tailed *t* test, and the significance of survival data was evaluated using the log-rank (Mantel-Cox) test. To compare three or more groups, one-way analysis of variance (ANOVA) with post-hoc Dunnett's multiple comparisons or the nonparametric Kruskal-Wallis test with post-hoc Dunn's test was used to determine statistical significance between groups. All statistical analyses were performed using GraphPad Prism software.

Reporting summary

Further information on research design is available in the Nature Portfolio Reporting Summary linked to this article.

Data availability

The data that support the findings of this study are available from the corresponding author upon reasonable request. Source data are provided with this paper.

References

1. Kershaw, M. H., Teng, M. W., Smyth, M. J. & Darcy, P. K. Supernatural T cells: genetic modification of T cells for cancer therapy. *Nat. Rev. Immunol.* **5**, 928–940 (2005).
2. Maude, S. L. et al. Chimeric antigen receptor T cells for sustained remissions in leukemia. *N. Engl. J. Med.* **371**, 1507–1517 (2014).
3. Gill, S. & Brudno, J. N. CAR T-Cell therapy in hematologic malignancies: Clinical role, toxicity, and unanswered questions. *Am. Soc. Clin. Oncol. Educ. Book* **41**, 1–20 (2021).
4. Rafiq, S., Hackett, C. S. & Brentjens, R. J. Engineering strategies to overcome the current roadblocks in CAR T cell therapy. *Nat. Rev. Clin. Oncol.* **17**, 147–167 (2020).
5. Lamers, C. H. et al. Treatment of metastatic renal cell carcinoma with CAIX CAR-engineered T cells: clinical evaluation and management of on-target toxicity. *Mol. Ther.* **21**, 904–912 (2013).
6. Morgan, R. A., Yang, J. C., Kitano, M., Dudley, M. E., Laurencot, C. M. & Rosenberg, S. A. Case report of a serious adverse event following the administration of T cells transduced with a chimeric antigen receptor recognizing ERBB2. *Mol. Ther.* **18**, 843–851 (2010).
7. Thistlethwaite, F. C. et al. The clinical efficacy of first-generation carcinoembryonic antigen (CEACAM5)-specific CAR T cells is limited by poor persistence and transient pre-conditioning-dependent respiratory toxicity. *Cancer Immunol. Immunother.* **66**, 1425–1436 (2017).
8. Roybal, K. T. et al. Precision tumor recognition by T cells with combinatorial antigen-Sensing Circuits. *Cell* **164**, 770–779 (2016).
9. Srivastava, S. et al. Logic-gated ROR1 chimeric antigen receptor expression rescues T cell-mediated toxicity to normal tissues and enables selective tumor targeting. *Cancer Cell* **35**, 489–503 e488 (2019).
10. Kloss, C. C., Condomines, M., Cartellieri, M., Bachmann, M. & Sadelain, M. Combinatorial antigen recognition with balanced signaling promotes selective tumor eradication by engineered T cells. *Nat. Biotechnol.* **31**, 71–75 (2013).
11. Lanitis, E. et al. Chimeric antigen receptor T Cells with dissociated signaling domains exhibit focused antitumor activity with reduced potential for toxicity in vivo. *Cancer Immunol. Res.* **1**, 43–53 (2013).
12. Fedorov, V. D., Themeli, M. & Sadelain, M. PD-1- and CTLA-4-based inhibitory chimeric antigen receptors (iCARs) divert off-target immunotherapy responses. *Sci. Transl. Med.* **5**, 215ra172 (2013).
13. Hoyos, V. et al. Engineering CD19-specific T lymphocytes with interleukin-15 and a suicide gene to enhance their anti-lymphoma/leukemia effects and safety. *Leukemia* **24**, 1160–1170 (2010).
14. Tasian, S. K. et al. Optimized depletion of chimeric antigen receptor T cells in murine xenograft models of human acute myeloid leukemia. *Blood* **129**, 2395–2407 (2017).
15. Paszkiewicz, P. J. et al. Targeted antibody-mediated depletion of murine CD19 CAR T cells permanently reverses B cell aplasia. *J. Clin. Invest.* **126**, 4262–4272 (2016).
16. Hong, M., Clubb, J. D. & Chen, Y. Y. Engineering CAR-T cells for next-generation cancer therapy. *Cancer Cell* **38**, 473–488 (2020).
17. Urbanska, K. et al. A universal strategy for adoptive immunotherapy of cancer through use of a novel T-cell antigen receptor. *Cancer Res.* **72**, 1844–1852 (2012).
18. Tamada, K. et al. Redirecting gene-modified T cells toward various cancer types using tagged antibodies. *Clin. Cancer Res.* **18**, 6436–6445 (2012).
19. Ma, J. S. et al. Versatile strategy for controlling the specificity and activity of engineered T cells. *Proc. Natl. Acad. Sci. USA* **113**, E450–E458 (2016).
20. Rodgers, D. T. et al. Switch-mediated activation and retargeting of CAR-T cells for B-cell malignancies. *Proc. Natl. Acad. Sci. USA* **113**, E459–E468 (2016).
21. Cho, J. H., Collins, J. J. & Wong, W. W. Universal chimeric antigen receptors for multiplexed and logical control of T cell responses. *Cell* **173**, 1426–1438.e1411 (2018).
22. Lee, Y. G. et al. Regulation of CAR T cell-mediated cytokine release syndrome-like toxicity using low molecular weight adapters. *Nat. Commun.* **10**, 2681 (2019).
23. Costello, R. T., Gastaut, J. A. & Olive, D. What is the real role of CD40 in cancer immunotherapy? *Immunol. Today* **20**, 488–493 (1999).
24. Grewal, I. S. & Flavell, R. A. CD40 and CD154 in cell-mediated immunity. *Annu. Rev. Immunol.* **16**, 111–135 (1998).
25. Hassan, S. B., Sorensen, J. F., Olsen, B. N. & Pedersen, A. E. Anti-CD40-mediated cancer immunotherapy: an update of recent and ongoing clinical trials. *Immunopharmacol. Immunotoxicol.* **36**, 96–104 (2014).
26. Vonderheide, R. H. CD40 Agonist antibodies in cancer immunotherapy. *Annu. Rev. Med.* **71**, 47–58 (2020).
27. Hollenbaugh, D. et al. Expression of functional CD40 by vascular endothelial cells. *J. Exp. Med.* **182**, 33–40 (1995).
28. Young, L. S., Eliopoulos, A. G., Gallagher, N. J. & Dawson, C. W. CD40 and epithelial cells: across the great divide. *Immunol. Today* **19**, 502–506 (1998).
29. Zhang, Y., Cao, H. J., Graf, B., Meekins, H., Smith, T. J. & Phipps, R. P. CD40 engagement up-regulates cyclooxygenase-2 expression and prostaglandin E2 production in human lung fibroblasts. *J. Immunol.* **160**, 1053–1057 (1998).
30. Neelapu, S. S. et al. Chimeric antigen receptor T-cell therapy - assessment and management of toxicities. *Nat. Rev. Clin. Oncol.* **15**, 47–62 (2018).
31. Norelli, M. et al. Monocyte-derived IL-1 and IL-6 are differentially required for cytokine-release syndrome and neurotoxicity due to CAR T cells. *Nat. Med.* **24**, 739–748 (2018).
32. Giavridis, T., van der Stegen, S. J. C., Eyquem, J., Hamieh, M., Piersigilli, A. & Sadelain, M. CAR T cell-induced cytokine release syndrome is mediated by macrophages and abated by IL-1 blockade. *Nat. Med.* **24**, 731–738 (2018).
33. Kim, H., Yoon, S. & Chung, J. In vitro and in vivo application of anti-cotinine antibody and cotinine-conjugated compounds. *BMB Rep.* **47**, 130–134 (2014).
34. Heo, K. et al. An aptamer-antibody complex (oligobody) as a novel delivery platform for targeted cancer therapies. *J. Control Release* **229**, 1–9 (2016).
35. Yu, B. et al. A hybrid platform based on a bispecific peptide-antibody complex for targeted cancer therapy. *Angew. Chem. Int. Ed. Engl.* **58**, 2005–2010 (2019).
36. Kang, H. Y. et al. A modifiable universal cotinine-chimeric antigen system of NK cells with multiple targets. *Front. Immunol.* **13**, 1089369 (2022).
37. Yoon, A., Shin, J. W., Kim, S., Kim, H. & Chung, J. Chicken scFvs with an artificial cysteine for site-directed conjugation. *PLoS One* **11**, e0146907 (2016).
38. Viaud, S. et al. Switchable control over in vivo CAR T expansion, B cell depletion, and induction of memory. *Proc. Natl. Acad. Sci. USA* **115**, E10898–E10906 (2018).
39. Greten, F. R. & Grivennikov, S. I. Inflammation and cancer: Triggers, mechanisms, and consequences. *Immunity* **51**, 27–41 (2019).
40. Weninger, W., Crowley, M. A., Manjunath, N. & von Andrian, U. H. Migratory properties of naive, effector, and memory CD8(+) T cells. *J. Exp. Med.* **194**, 953–966 (2001).
41. Hess, P. R. et al. Selective deletion of antigen-specific CD8+ T cells by MHC class I tetramers coupled to the type I ribosome-inactivating protein saporin. *Blood* **109**, 3300–3307 (2007).
42. Vincent, B. G. et al. Toxin-coupled MHC class I tetramers can specifically ablate autoreactive CD8+ T cells and delay diabetes in nonobese diabetic mice. *J. Immunol.* **184**, 4196–4204 (2010).
43. Palchaudhuri, R. et al. Non-genotoxic conditioning for hematopoietic stem cell transplantation using a hematopoietic-cell-specific internalizing immunotoxin. *Nat. Biotechnol.* **34**, 738–745 (2016).

44. Persaud, S. P. et al. Antibody-drug conjugates plus Janus kinase inhibitors enable MHC-mismatched allogeneic hematopoietic stem cell transplantation. *J. Clin. Invest.* **131**, e145501 (2021).
45. Brudno, J. N. et al. Allogeneic T cells that express an anti-CD19 chimeric antigen receptor induce remissions of B-cell malignancies that progress after allogeneic hematopoietic stem-cell transplantation without causing graft-versus-host disease. *J. Clin. Oncol.* **34**, 1112–1121 (2016).
46. Chen, Y. et al. Donor-derived CD19-targeted T cell infusion induces minimal residual disease-negative remission in relapsed B-cell acute lymphoblastic leukaemia with no response to donor lymphocyte infusions after haploidentical haematopoietic stem cell transplantation. *Br. J. Haematol.* **179**, 598–605 (2017).
47. Jacoby, E., Yang, Y., Qin, H., Chien, C. D., Kochenderfer, J. N. & Fry, T. J. Murine allogeneic CD19 CAR T cells harbor potent antileukemic activity but have the potential to mediate lethal GVHD. *Blood* **127**, 1361–1370 (2016).
48. Ghosh, A. et al. Donor CD19 CAR T cells exert potent graft-versus-lymphoma activity with diminished graft-versus-host activity. *Nat. Med.* **23**, 242–249 (2017).
49. Liu, X. et al. Affinity-tuned ErbB2 or EGFR chimeric antigen receptor T cells exhibit an increased therapeutic index against tumors in mice. *Cancer Res.* **75**, 3596–3607 (2015).
50. Park, S. et al. Micromolar affinity CAR T cells to ICAM-1 achieves rapid tumor elimination while avoiding systemic toxicity. *Sci. Rep.* **7**, 14366 (2017).
51. Castellarin, M. et al. A rational mouse model to detect on-target, off-tumor CAR T cell toxicity. *JCI Insight* **5**, e136012 (2020).
52. Juillerat, A. et al. Modulation of chimeric antigen receptor surface expression by a small molecule switch. *BMC Biotechnol.* **19**, 44 (2019).
53. Richman, S. A., Wang, L. C., Moon, E. K., Khire, U. R., Albelda, S. M. & Milone, M. C. Ligand-induced degradation of a CAR permits reversible remote control of CAR T cell activity in vitro and in vivo. *Mol. Ther.* **28**, 1600–1613 (2020).
54. Jan, M. et al. Reversible ON- and OFF-switch chimeric antigen receptors controlled by lenalidomide. *Sci. Transl. Med.* **13**, eabb6295 (2021).
55. Labanieh, L. et al. Enhanced safety and efficacy of protease-regulated CAR-T cell receptors. *Cell* **185**, 1745–1763.e1722 (2022).
56. Pishali Bejestani, E. et al. Characterization of a switchable chimeric antigen receptor platform in a pre-clinical solid tumor model. *Oncoimmunology* **6**, e1342909 (2017).
57. Adams, R. et al. Extending the half-life of a fab fragment through generation of a humanized anti-human serum albumin Fv domain: An investigation into the correlation between affinity and serum half-life. *MAbs* **8**, 1336–1346 (2016).
58. Wermke, M. et al. Proof of concept for a rapidly switchable universal CAR-T platform with UniCAR-T-CD123 in relapsed/refractory AML. *Blood* **137**, 3145–3148 (2021).
59. Li, D. K. & Wang, W. Characteristics and clinical trial results of agonistic anti-CD40 antibodies in the treatment of malignancies. *Oncol. Lett.* **20**, 176 (2020).
60. Bonnans, C. et al. CD40 agonist-induced IL-12p40 potentiates hepatotoxicity. *J. Immunother. Cancer* **8**, e000624 (2020).
61. Chiodoni, C. et al. Triggering CD40 on endothelial cells contributes to tumor growth. *J. Exp. Med.* **203**, 2441–2450 (2006).
62. Vowinkel, T., Wood, K. C., Stokes, K. Y., Russell, J., Krieglstein, C. F. & Granger, D. N. Differential expression and regulation of murine CD40 in regional vascular beds. *Am. J. Physiol. Heart Circ. Physiol.* **290**, H631–H639 (2006).
63. Guo, M. et al. Guided construction of single cell reference for human and mouse lung. *Nat. Commun.* **14**, 4566 (2023).
64. Orfanos, S. E., Mavrommati, I., Korovesi, I. & Roussos, C. Pulmonary endothelium in acute lung injury: from basic science to the critically ill. *Intensive Care Med.* **30**, 1702–1714 (2004).
65. Kuhn, N. F. et al. CD40 Ligand-modified chimeric antigen receptor T cells enhance antitumor function by eliciting an endogenous antitumor response. *Cancer Cell* **35**, 473–488.e476 (2019).
66. Riah, O., Dousset, J. C., Courriere, P., Stigliani, J. L., Baziard-Mouysset, G. & Belahsen, Y. Evidence that nicotine acetylcholine receptors are not the main targets of cotinine toxicity. *Toxicol. Lett.* **109**, 21–29 (1999).
67. Tan, X., Vrana, K. & Ding, Z. M. Cotinine: Pharmacologically active metabolite of nicotine and neural mechanisms for its actions. *Front. Behav. Neurosci.* **15**, 758252 (2021).
68. Khongorzul, P., Ling, C. J., Khan, F. U., Ihsan, A. U. & Zhang, J. Antibody-drug conjugates: A comprehensive review. *Mol. Cancer Res.* **18**, 3–19 (2020).
69. Andris-Widhopf, J., Steinberger, P., Fuller R., Rader, C. & Barbas, C. F. 3rd Generation of human scFv antibody libraries: PCR amplification and assembly of light- and heavy-chain coding sequences. *Cold Spring Harb. Protoc.* **2011**, pdb.prot065573 (2011).
70. Kochenderfer, J. N., Yu, Z., Frasheri, D., Restifo, N. P. & Rosenberg, S. A. Adoptive transfer of syngeneic T cells transduced with a chimeric antigen receptor that recognizes murine CD19 can eradicate lymphoma and normal B cells. *Blood* **116**, 3875–3886 (2010).
71. Park, S., Lee, D. H., Park, J. G., Lee, Y. T. & Chung, J. A sensitive enzyme immunoassay for measuring cotinine in passive smokers. *Clin. Chim. Acta* **411**, 1238–1242 (2010).
72. Kochenderfer, J. N. et al. Eradication of B-lineage cells and regression of lymphoma in a patient treated with autologous T cells genetically engineered to recognize CD19. *Blood* **116**, 4099–4102 (2010).
73. Chakraverty, R. et al. Host MHC class II+ antigen-presenting cells and CD4 cells are required for CD8-mediated graft-versus-leukemia responses following delayed donor leukocyte infusions. *Blood* **108**, 2106–2113 (2006).
74. Li, H. W., Sachs, J., Pichardo, C., Bronson, R., Zhao, G. & Sykes, M. Nonalloreactive T cells prevent donor lymphocyte infusion-induced graft-versus-host disease by controlling microbial stimuli. *J. Immunol.* **189**, 5572–5581 (2012).

Acknowledgements

We thank Prof. Aesun Shin (Seoul National University College of Medicine) for statistical advice. Cartoons of experimental mice in figures were created in BioRender (Choi, K. (2024) BioRender.com/v13c533). This research was supported by the Bio & Medical Technology Development Program of the National Research Foundation (NRF) funded by the Ministry of Science & ICT (MSIT), Republic of Korea (2016M3A9D3900438), the Korea Drug Development Fund (KDDF) funded by the MSIT, Ministry of Trade, Industry and Energy, and Ministry of Health and Welfare, Republic of Korea (HN21C0764), and the Innovation Research Center (IRC) grant of the NRF funded by the MSIT, Republic of Korea (RS-2023-00260454).

Author contributions

S.J.C., J.C., and K.C. designed and supervised the experiments. H.B.P., K.H.K., J.H.K., S.I.K., Y.M.O., M.K., S.L., S.H., H.L., T.L., S.P., J.E.L., and G.R.J. performed the experiments. H.Y. and E.Y.C. participated in the design and construction of the effluc-CAR. D.H.L and W.C.S. examined histology slides from CAR-T cell-treated mice. H.B.P. and K.C. wrote the manuscript.

Competing interests

K.C. and E.Y.C. are founders and shareholders of Ticaros Inc. H.B.P., J.E.L., and G.R.J. are currently employees of Ticaros. K.C., J.C., H.B.P., K.H.K., S.I.K., and G.R.J. are co-inventors on the pending patent for anti-CD40 switchable CAR T cells. The other authors declare no competing interests.

Additional information

Supplementary information The online version contains supplementary material available at https://doi.org/10.1038/s41467-024-53996-7.

Correspondence and requests for materials should be addressed to Sang J. Chung, Junho Chung or Kyungho Choi.

Peer review information Nature Communications thanks Damya Laoui and the other anonymous reviewer(s) for their contribution to the peer review of this work. A peer review file is available.